SITE CLASSIFICATION OF TURKISH NATIONAL STRONG-MOTION RECORDING SITES

A THESIS SUBMITTED TO
THE GRADUATE SCHOOL OF NATURAL AND APPLIED SCIENCES
OF
MIDDLE EAST TECHNICAL UNIVERSITY

BY

MUSTAFA ABDULLAH SANDIKKAYA

IN PARTIAL FULFILLMENT OF THE REQUIREMENTS
FOR
THE DEGREE OF MASTER OF SCIENCE
IN
CIVIL ENGINEERING

JULY 2008

Approval of the thesis:

SITE CLASSIFICATION OF TURKISH NATIONAL STRONG-MOTION RECORDING SITES

submitted by **MUSTAFA ABDULLAH SANDIKKAYA** in partial fulfillment of the requirements for the degree of **Master of Science in Civil Engineering Department, Middle East Technical University** by,

Prof. Dr. Canan Özgen
Dean, Graduate School of **Natural and Applied Sciences** _____

Prof. Dr. Güney Özcebe
Head of Department, **Civil Engineering** _____

Assoc. Prof. Dr. B. Sadık Bakır
Supervisor, **Civil Engineering Dept., METU** _____

Assist. Prof. Dr. M. Tolga Yılmaz
Co-supervisor, **Engineering Sciences Dept., METU** _____

Examining Committee Members:

Prof. Dr. Polat Gülkan
Civil Engineering Dept., METU _____

Assoc. Prof. Dr. B. Sadık Bakır
Civil Engineering Dept., METU _____

Assist. Prof. Dr. M. Tolga Yılmaz
Engineering Sciences Dept., METU _____

Assoc. Prof. Dr. Sinan Akkar
Civil Engineering Dept., METU _____

Assoc. Prof. Dr. Özdoğan Yılmaz
Anatolian Geophysical _____

Date: 28.07.2008

I hereby declare that all information in this document has been obtained and presented in accordance with academic rules and ethical conduct. I also declare that, as required by these rules and conduct, I have fully cited and referenced all material and results that are not original to this work.

Name, Last name: Mustafa Abdullah SANDIKKAYA

Signature :

ABSTRACT

SITE CLASSIFICATION OF TURKISH NATIONAL STRONG-MOTION RECORDING SITES

SANDIKKAYA, Mustafa Abdullah
M.Sc., Department of Civil Engineering
Supervisor : Assoc. Prof. Dr. B. Sadık BAKIR
Co-Supervisor : Assist. Prof. Dr. M. Tolga YILMAZ

July 2008, 94 Pages

Since 1976, the General Directorate of Disaster Affairs of Turkey has deployed several strong-motion accelerographs at selected sites. Within the framework of the project entitled Compilation of National Strong Ground Motion Database in Accordance with International Standards, initiated in 2006, site conditions at a total of 153 strong-motion sites were investigated within the uppermost 30 m depth through boreholes including Standard Penetration Testing and surface seismics by means of Multi-channel Analysis of Surface Waves (MASW). In this study, firstly, the assessment of the site characterization was held by making use NEHRP Provisions, EC-8 and Turkish Seismic Design Code. The corrected penetration resistances are calculated and observed how it affects the classification. In addition, the consistency of site classes obtained from either penetration resistance or shear wave velocity criteria is examined. Also the consistency of the boundaries of the site classes in terms of shear wave velocity and

penetration resistance data pairs are investigated. Secondly, the liquefaction potential of these sites is examined. Thirdly and finally, the shear wave velocity profiles obtained from MASW technique are contrasted to other seismic tests.

Keywords: Site classification, strong ground motion, shear wave velocity, standard penetration resistance and seismic hazard

ÖZ

TURK ULUSAL KUVVETLİ YER HAREKETİ KAYIT İSTASYONLARININ ZEMİN SINIFLANDIRMASI

SANDIKKAYA, Mustafa Abdullah
Yüksek Lisans, İnşaat Mühendisliği Bölümü
Tez Yöneticisi : Doç. Dr. B. Sadık BAKIR
Ortak Tez Yöneticisi : Yrd. Doç. Dr. M. Tolga YILMAZ

Temmuz 2008, 94 sayfa

Afet İşleri Genel Müdürlüğü 1976'dan beri seçilmiş birçok sahaya kuvvetli yer haraketi kayıt cihazları yerleştirmiştir. 2006 yılında başlanan 'Ulusal Kuvvetli Yer Haraketleri Kayıt Şebekesi Veritabanının Uluslararası Ölçütlere Göre Derlenmesi' projesi kapsamında, 153 kuvvetli yer hareketi kayıt istasyonu lokasyonunda 30 m derinlik içerisindeki yerel saha koşulları Standart Penetrasyon Deneyi (SPT) ve Yüzey Dalgalarının Çok Kanallı Analizi (MASW) ile incelenmiştir. Bu çalışmada, ilk olarak saha sınıflandırmasının değerlendirilmesi NEHRP, EC-8 ve Türk Deprem Şartnamelerine göre yapılmıştır. Düzeltilmiş SPT darbe sayıları hesaplanmış ve zemin sınıflandırmasına etkisi gözlemlenmiştir. Buna ek olarak, SPT darbe sayısı ve kayma dalga hızı yaklaşımlarına göre belirlenen saha sınıflarının tutarlılığı incelenmiştir. Ayrıca SPT darbe sayısı ile kayma dalga hızı verilerinin zemin sınıfları sınır değerlerine göre tutarlılığı da değerlendirilmiştir. İkinci olarak, bu sahaların sıvılaşma

potasiyeli incelenmiştir. Üçüncü ve son olarak, MASW tekniği ile elde edilmiş kayma dalga hız profilleri diğer sismik testlerle elde edilmiş sonuçlar ile karşılaştırılmıştır.

Anahtar Kelimeler: Zemin sınıflandırması, kuvvetli yer haraketi, kayma dalgası hızı, standart penetrasyon deneyi, sismik tehlike

To My Family

ACKNOWLEDGMENTS

I would like to express my sincere gratitude to my supervisor Dr. B. Sadık Bakır and co-supervisor Dr. M. Tolga Yılmaz for their support, guidance, advice, criticism, encouragement and insight throughout our studies.

I also would like to express my faithful gratitude to Dr. Sinan Akkar for his leadership in the project besides his mastering thoughts to instruct and guide me throughout our studies.

This study is funded by the Scientific and Technological Research Council of Turkey (TUBITAK) under Award No. 105G016.

I would like to particularly thank Dr. Özdoğan Yılmaz and Erdoğdu Savaşkan (M.Sc.) for their help, comments and suggestions on the raw data that is used in this study.

I am grateful to Emrah Yenier and Özgür Erdoğan for their friendship, encouragement and support since we started to work together in the project. Besides, I would like to thank Özkan Kale and B. Özer Ay for their friendship and support.

I would like to thank to my office-mates, Yeşim Sema Ünsever and Zeynep Çekinmez for their friendship and understanding.

I wish to thank to Halil Soylu, Tan Sevim, Haluk Demirörs, Hakan Kırbıyık and others in “adamım@CE2005”.

Finally, I would like give my endless love to my family for their encouragement, unyielding patience and understanding throughout my life.

TABLE OF CONTENTS

LIST OF TABLES

TABLES

LIST OF FIGURES

FIGURES

LIST OF ABBREVATIONS

a_{crt}	critical peak ground acceleration
a_{max}	peak horizontal acceleration at ground surface
BHS	borehole seismic test
btw	between
C_B	correction factor for borehole diameter
C_E	correction factor for energy efficiency of hammer
C_N	correction factor for the overburden pressure
C_R	correction factor for rod length
CRR	cyclic resistance ratio
C_S	correction factor for standard sampler
CSL	center of seismic line
CSR	cyclic stress ratio
dist	distance
EC-8	Eurocode 8 (CEN, 2003)
exp	exploration
FC	fines content
g	gravitational acceleration

GDDA	General Directorate of Disaster Affairs of Turkey
GWL	ground water level
h_1	topmost layer thickness
MASW	Multi-channel Analysis of Surface Waves
min	minimum
M_w	Moment magnitude
N	number of blow counts or penetration resistance
N_{60}	energy efficiency corrected penetration resistance
N_i	penetration resistance of the i^{th} layer
N_{mean}	mean penetration resistance of uppermost 30 m
$(N_1)_{60}$	completely corrected penetration resistance
$(N_1)_{60cs}$	penetration resistance of clean sands
$(N_{mean})_{1,60}$	mean penetration resistance with complete SPT correction of uppermost 30 m
$(N_{mean})_{60}$	mean penetration resistance with energy efficiency correction of uppermost 30 m
NEHRP	(NEHRP Provisions) National Earthquake Hazard Reduction Program Recommended Provisions (BSSC, 2003)
NSMP	Compilation of National Strong Ground Motion Database in Accordance with International Standards
NSMR-sites	National Strong-motion Recording Sites

PI	plasticity index
P-wave	Primary wave
q_u	undrained compressive strength
r_d	stress reduction factor
SASW	Spectral Analysis of Surface Waves
seis	seismograph
SPT	standard penetration test
S_u	undrained shear strength
$S_{u,30}$	mean undrained shear strength of uppermost 30 m
TSDC	Turkish Seismic Design Code (GDDA, 2007)
UCL	upper confidence limit
USCS	Unified Soil Classification System
V_p	Primary-wave velocity
V_s	shear wave velocity
$V_{s,30}$	mean shear wave velocity of uppermost 30 m
$V_{s,BHS}$	mean Vs obtained through BHS Method
$V_{s,MASW}$	mean Vs obtained through MASW method
$V_{s,SASW}$	mean Vs obtained through SASW method
V_{si}	shear wave velocity of the i^{th} layer

w	water content
z	depth below ground surface
α	coefficient for clean sand correction
β	coefficient for clean sand correction
σ_v'	effective vertical overburden stress
σ_v	total vertical overburden stress

CHAPTER 1

INTRODUCTION

1.1 General

One of the most seismotectonically active regions in the world is the Anatolian Peninsula, where a large number of destructive earthquakes occurred within the past century. To monitor such earthquakes, General Directorate of Disaster Affairs of Turkey (GDDA) has deployed several strong-motion accelerographs near identified seismic sources.

The research project, Compilation of National Strong Ground Motion Database in Accordance with International Standards, undertaken by the collaboration of Civil Engineering Department of the Middle East Technical University (METU) and the Earthquake Research Department of GDDA and funded by The Scientific and Technological Research Council of Turkey, (TÜBİTAK) aims at examination and categorization of the properties of earthquake database that are collected by GDDA since 1976. The first task is to order the accelerometric data and then to compile events and records. The second task is to gather the event information, such as epicenteral coordinates, depths, magnitudes, source parameters, from international agencies and institutes, and then to calculate distances to strong motion accelerograph stations. The third task is to process the records according to their qualities and properties (Erdoğan, 2008).

It is necessary to know the local site conditions in order to characterize the strong-motion records. For this reason, geophysical and geotechnical tests were performed at a total of 153 national strong-motion recording sites (NSMR-sites) within the research project. In addition, the borehole seismic test is performed on 9 selected sites. The shear wave velocity and penetration resistance profiles presented in this study are acquired from the project interim reports submitted by the contractors. References to these reports are given as:

- TÜBİTAK Research Project, No. 105G016, Compilation of Data Base for the National Strong Motion Seismograph Network in Turkey, Report on Seismic and Geotechnical Investigations, 2007, Department of Civil Engineering, Middle East Technical University

- TÜBİTAK Research Project, No. 105G016, Compilation of Data Base for the National Strong Motion Seismograph Network in Turkey, Report on Borehole Seismic Investigations, 2008, Department of Civil Engineering, Middle East Technical University

1.2 Literature Survey

The ground motion parameters depend on site response. The site response is related with the depth to bedrock, type of deposits and properties of materials (Bullen, 1965, Aki and Richards, 1980, Steward et al., 2001, and Rodriguez-Marek et al., 2001). Consequently, engineers need to know response of soil media in order to build structures that are capable of withstanding the seismic loads. In order to obtain a simple approach to quantify the site effects on design loads, the sites which show similar dynamic response to seismic excitation are grouped as site classes, so that severity of seismic loads can be defined for each class (Dobry et al., 2000, Lee et al., 2001, and Rathje et al., 2003). Mexico City 1985, Loma Prieta

1989, Chi-Chi 1999, Adapazarı 1999 and Düzce 1999 earthquakes showed the importance of the local site effects (Dobry et al., 2000, Rodriguez-Marek et al., 2001 and Rathje et al. 2003).

One of the earliest site classification studies is presented by Seed et al. (1976). Seed et al. proposed spectrum shapes for different site conditions using 104 strong motion records with peak acceleration greater than 0.05g. Sites are classified as either rock (28 records) or stiff soil (31 records) or deep cohensionless soil (30 records) or soft to medium clay and sand (15 records). For 5% structural damping, mean and mean-plus-one standard deviation normalized acceleration response spectra of these records are obtained. Figure 1.1 shows the mean normalized acceleration spectra for the four site classes.

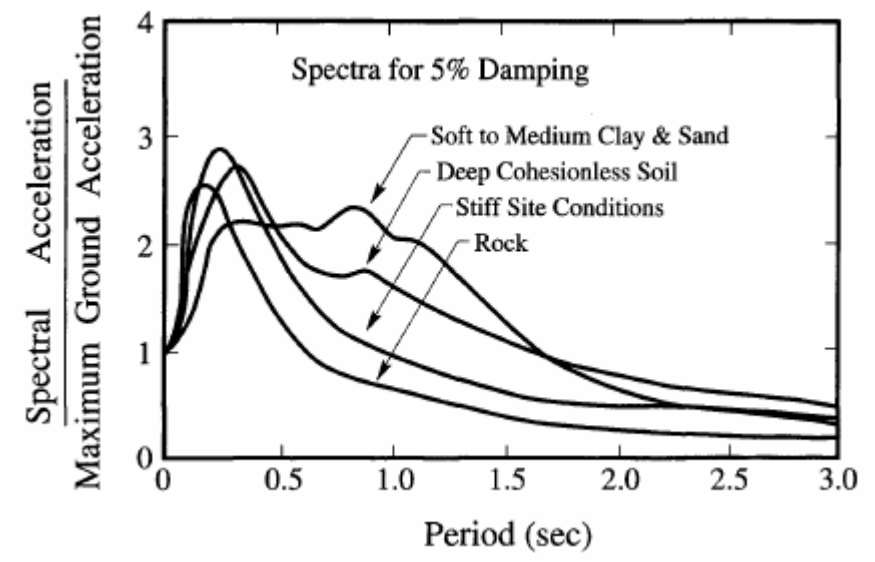

Figure 1.1 The mean acceleration spectra for different site conditions (Seed et al. 1976)

A site classification system which is similar to that given by Seed et al., 1976 was used prior to 1994 NEHRP Provisions. Later, site classes of which definitions given in Table 1.1 were developed with geotechnical and geophysical data to characterize site conditions. For classification, three types of information can be used: (1) Descriptions of the shallow lithology according to Table 1.1, (2) mean shear wave velocity of uppermost 30 m of soil/rock profile, which is estimated through employing correlations with layer and formation definitions, (3) mean shear wave velocity of uppermost 30 m which is equal to 30 m divided by total travel time of vertically incident shear waves from depth of 30 m to ground surface (Borcherdt, 1994). The first type of information can be gathered from available geological maps, whereas the second type can be obtained by borings and the third requires seismic tests.

Table 1.1 Site class definitions suggested by Borcherdt (1994)

Site Class	Description of layers	V_s (m/s)
SC- I	Hard to firm rock	> 700
SC- II	Gravelly soils and soft rock	375-700
SC- III	Stiff clays and sandy soils	200-375
SC- IV	Soft soils	<200

The 1994 version of NEHRP Provisions employed the site class definitions that are still in use. Mean shear velocity profiles of the sites are introduced and primarily taken into account to classify the local site conditions (Dobry

et al., 2000). Site classification, based on representative mean shear wave velocity of the uppermost 30 m, provides the most accurate site characterization. This method solely considered the top 30 m of soil, disregarding the material deposited below 30 m depth (Dobry et al., 2000). Shear wave velocity, penetration resistance or undrained shear strength can be used for site classification. Consequently, the requirement of consistency between geotechnical and geophysical properties is mandatory (Borcherdt, 1994).

The seismic design code used in Europe (EC-8) is based on the same methodology with NEHRP Provisions, except for a minor difference between class definitions for rock sites. On the other hand, the seismic design code in Turkey has a different methodology. Turkish site classification scheme is primarily based on the lithologic information used with information on either shear wave velocity or penetration resistance or unconfined compression strength of shallow layers. Turkish site classes are established in the code published in 1975 and are still in use in current edition.

In the literature there are some other methods that are used for site classification. Rodriguez-Marek et al. (2001) introduced a new site classification system which primarily based on type of deposit and depth to bedrock. Also, depositional age and soil type used as secondary parameters. Zare and Bard (2002) classified the sites in Turkey with the horizontal to vertical spectral ratio method which is applied to strong-motion records. Kim and Yoon (2006) proposed using the site period that is calculated by the shear wave velocity to the bedrock depth. Phung et al. (2006) classified the sites in Taiwan by response spectral shape method. In this method, the normalized spectra of records were obtained to determine the predominant periods.

In NEHRP provisions and EC-8, special sites that require site specific response analysis are addressed, after lessons from Mexico City 1985 and Loma Prieta 1989 earthquakes (Dobry et al., 2000). The response of sites that involve thick soft soils, involving liquefiable deposits, is strongly related to the amplitude of the ground motion, due to the excessive nonlinear soil behavior. Similar observations in Adapazarı are reported by Bakır et al (2005) after Adapazarı 1999 earthquake. Besides, sites with very thick medium stiff clays and with shallow soft deposits underlain by rock are other cases that require specific analysis. The characteristics of ground motion on these sites are strongly dependent on total thickness of soil deposits (Kramer, 1996, Rathje et al. 2003, and Kim and Yoon, 2006).

1.3 Objective and Scope

In this study, utilizing the available data from geophysical and geotechnical tests, the NSMR-sites are classified according to:

- National Earthquake Hazard Reduction Program Recommended Provisions for Seismic Regulations for New Buildings and Other Structures, Part 1: Provisions ~ NEHRP Provisions ~ (BSSC, 2003)

- Eurocode-8, Design of structures for earthquake resistance – Part1: General rules, seismic actions and rules for buildings ~ EC-8 ~ (CEN, 2003)

- Turkish Seismic Design Code: Specification for Structures to be Built in Disaster Areas ~ TSDC ~ (GDDA, 2007).

The liquefaction susceptibility of sites is determined with the simplified procedure given by Youd et al. (2001).

In Chapter 1, a literature survey on site classification and scope of the study is presented. In Chapter 2, general information on the NSMR-sites and brief information on the conducted seismic and geotechnical tests are provided. In Chapter 3, the NSMR-sites are classified according to the earthquake codes in use. Special emphasis is put on the effect of penetration resistance correction on site classification. In addition, the consistency between the seismic and geotechnical criteria for site classes is investigated. In Chapter 4, the liquefaction susceptibility of NSMR-sites is evaluated. In Chapter 5, the data from three different seismic test types are compared for selected sites. Finally the summary and conclusions of this study are presented in Chapter 6.

CHAPTER 2

THE NSMR-SITES AND SITE INVESTIGATONS

2.1 The NSMR-Sites

The site conditions at the NSMR-sites were investigated by surface seismic and Standard Penetration Tests. Figure 2.1 shows the locations of the NSMR-sites on Turkey.

Figure 2.1 The NSMR sites in Turkey (Yılmaz et al. 2008b)

The NSMR-sites and their locations are listed, according to the station codes referred in the project, Compilation of National Strong Ground Motion Database in Accordance with International Standards (NSMP) and the station abbreviations used by GDDA in Appendix A. Figure 2.2 shows a representative plan of site investigations. Besides, the seismograph, the center of seismic line and borehole coordinates, and the distances between these three points are also given in Appendix A. The histogram for distance between these points is provided in Figure 2.3. The center of seismic line is the mid-point of the 94 m receiver cable which was used in surface seismic surveys. The altitudes of stations, ground water levels, mean representative values of shear wave velocity and penetration resistance (based on MASW and SPT results), and the respective site classes, determined as explained in Chapter 3, are also presented in Appendix A.

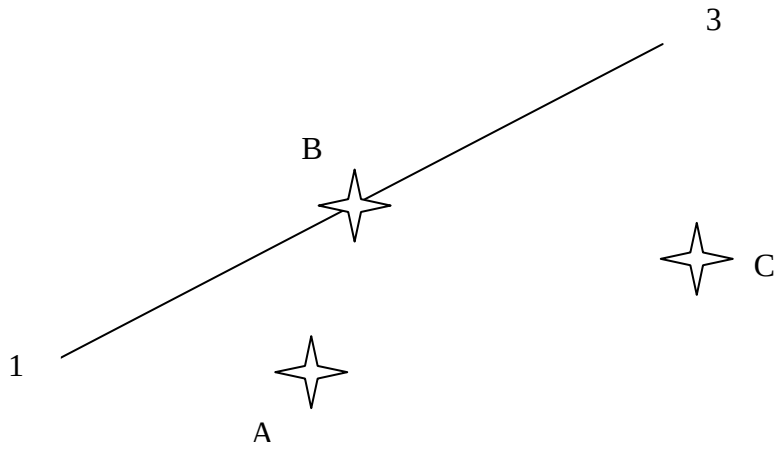

Figure 2.2 Typical site investigation plan view: Line 1-3 is the seismic line, point A is the seismograph station, point B is the center point of the seismic line, and point C is the borehole location

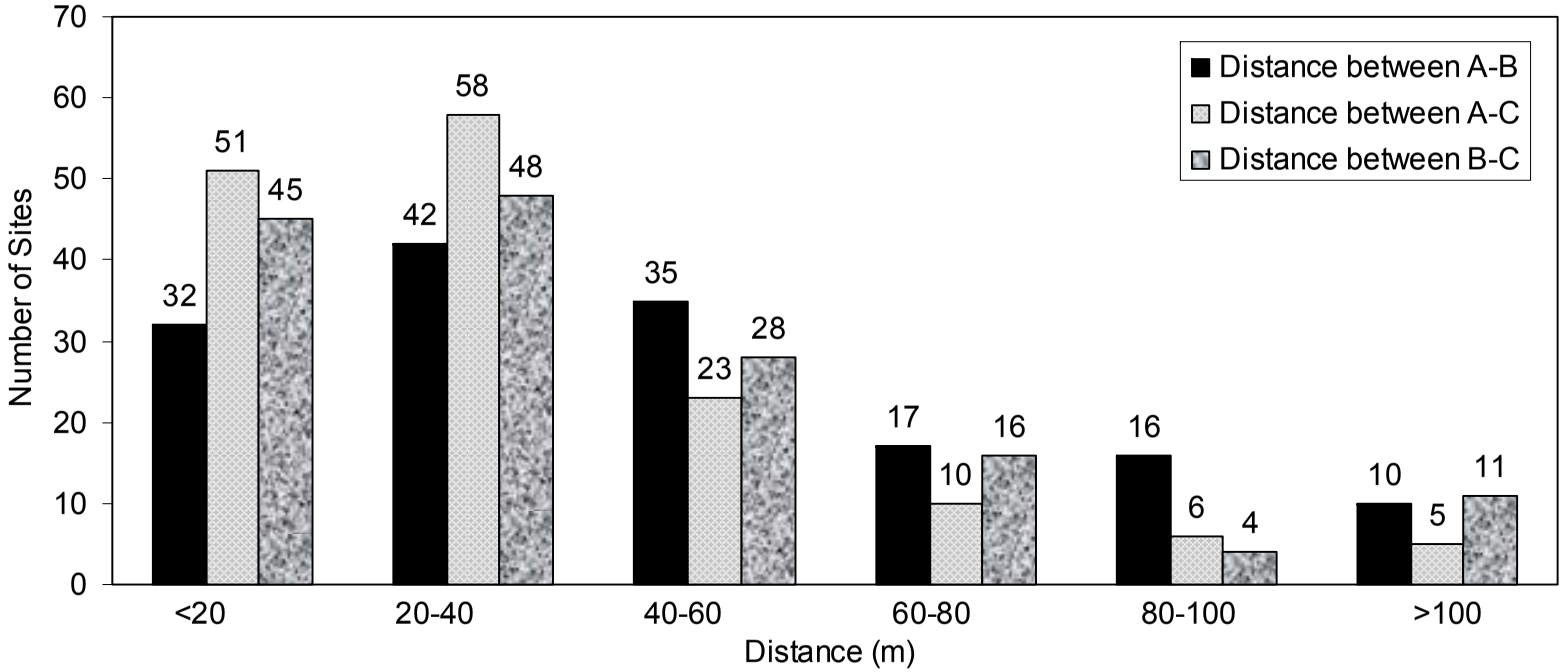

Figure 2.3 The histogram of distances between the points shown in Figure 2.1

2.2 Determination of the Soil Properties

One of the most popular in-situ tests in geotechnical practice is the standard penetration test (SPT). During the test, the 63.5 kg-hammer is dropped from 76 cm height in order to drive the sampler tube 15 cm into the soil located at the end of a borehole. The procedure is repeated continuously 3 times at a specific depth. The number of hammer blows required to drive the sampler for each 15 cm is recorded. The penetration resistance N is the number of blows required to drive the sampler in the last (2x15) 30 cm of soil. In SPT, when 50 blows are reached for any 15 cm penetration the test is halted and the “refusal” is indicated on the borelog by noting the total length of penetration in soil corresponding to 50 blows.

Result of a SPT depends on type of deposit, depth, geological age and testing equipment. For example, the energy efficiency of the hammer could vary from one country to another due to the different triggering mechanisms. In some geotechnical applications, the results of SPT are usually corrected before employing in geotechnical assessment and foundation design.

Furthermore, soil layers are identified in situ by visually investigating the properties of the material coming out of the borehole. During the test, disturbed samples are retrieved by split-spoon sampler and such are used for classification tests including sieve analysis, and to determine water content and Atterberg limits of soils. By these tests, particle size distribution, natural water content (w), liquid limit (LL), plastic limit (PL), plasticity index (PI) of soil were obtained. Employing these parameters, soil classification was made according to the Unified Soil Classification System (USCS).

SPT is not applicable in gravels and rocks (weathered or intact) due to low relative size of the sampler diameter with respect to the particle size of the sample. Hence, in case a rock layer was encountered, core samples were recovered. Total core recovery (TCR) and rock quality designation (RQD) values of the rock cores were reported where applicable (Yılmaz et al., 2008b).

For cohesive soils, if available, the undisturbed samples were taken with Shelby tubes in order to carry out unconfined compression tests in the laboratory. Undrained compressive strength (q_u) and undrained shear strength ($S_u = q_u/2$) of the soil is determined from these tests.

2.3 Determination of Shear Wave Velocity Profiles

The shear wave velocity (V_s) profile can be obtained from seismic tests employing surface seismic and seismic downhole methods.

2.3.1 Surface Seismic Tests

In seismic tests, seismic sources can emit two types of waves: body and surface waves. Rayleigh wave is a type of surface wave, including both vertical and horizontal displacements which are out of phase by 90º on the surface of an elastic half-space (Kramer, 1996). Approximately two-thirds of the energy obtained from a vertical seismic source in a surface seismic survey is transmitted by Rayleigh wave (Park et al., 1999). The mechanical characteristics of Rayleigh waves can be used for determination of V_s profile of a site.

The first method developed for the purpose is the method of Spectral Analysis of Surface Waves (SASW) presented by Nazarian and Stokoe (1983 quoted by Park et al., 1997 and 1999). The dependency of phase

velocity to frequency of oscillations results in dispersion of waveforms. A dispersion curve is the plot of phase velocity versus frequency of oscillations. SASW is carried out by utilizing two receivers to record the surface motions at two points, and then by comparing the computed dispersion curve for Rayleigh wave with the theoretical. An accurate estimation of actual dispersion curve needs a series of configuration of receivers, increasing the costs. It is also difficult to remove noise from the records when only two receivers are used.

The second method, which aims to overcome the problems of SASW method by employing multiple receivers, is the method of Multichannel Analysis of Surface Waves (MASW). Simultaneous multichannel recordings have advantages in effective identification of dispersion curve, isolation of noise, and speed of tests (Park et al., 1997 and 1999).

The V_s profile can be estimated by three-step procedure; acquisition of dispersive ground displacement history, construction of dispersion curve, and inversion of dispersion curve, which finally provides V_s profile. The determination of a precise dispersion curve is essential in order to obtain V_s profile precisely. The dispersion of Rayleigh waves is predominantly due to the heterogeneity of V_s of soil profile. Hence, the layer thickness and V_s of each layer is properly chosen so that the theoretical dispersion curve for the fundamental frequency of Rayleigh wave agrees with the experimental results. The iterative procedure, namely the inversion continues until the best agreement between the theoretical and experimental dispersion curves are obtained (Kramer, 1996, Park et al., 1997 and 1999, Xia et al., 1999, 2003 and 2004).

The V_s profile of each NSMR-site is determined by employing MASW method. Detailed work can be found in the project interim reports however,

the executive summary of the procedure is presented in the following section.

2.3.1.1 Field tests

Field work of MASW method is very complicated and an extensive care must be given. The system involves an impact source, cables, geophones and seismic recording units. Figure 2.4 displays the diagram for field survey. An impact source is supplied by an electromechanically accelerated hammer of mass 50 kg. The generated waves are monitored with 48 4.5 Hz vertical geophones at 2 m interval attached to a 94 m long 48-channel receiver cable. The digital data transferred from two 24-channel GEODE recording unit to a computer for analysis.

Three sets of shots were performed at 2 m offset from the start and end points of receiver cable (pt 1 and pt 3 in Figure 2.5) and at the center of receiver cable (pt 2 in Figure 2.5). For each set one shot was applied as a vertical impact load to determine the primary wave (P-wave) velocity profile, and two shots were applied as horizontal impact loads to determine the V_s profile.

2.3.1.2 Computations

The records are used for selecting the first arrival times. Utilizing the nonlinear travel time tomography the initial V_p-depth model was derived (Zhang and Töksöz, 1999, quoted by Yılmaz et al., 2008b). The final laterally averaged V_p-depth model was computed by iterations. The records were usually contaminated with both refracted and reflected waves, and with ambient noise. The contamination of records is eliminated by isolating the waves by inside and outside mute and also applying band-pass filtering (Yılmaz et al., 2008b). The dispersion curve of the fundamental mode is

picked from dispersion spectrum obtained by plane wave decomposition. The initial V_s profile is estimated and final V_s profile is computed by iterations.

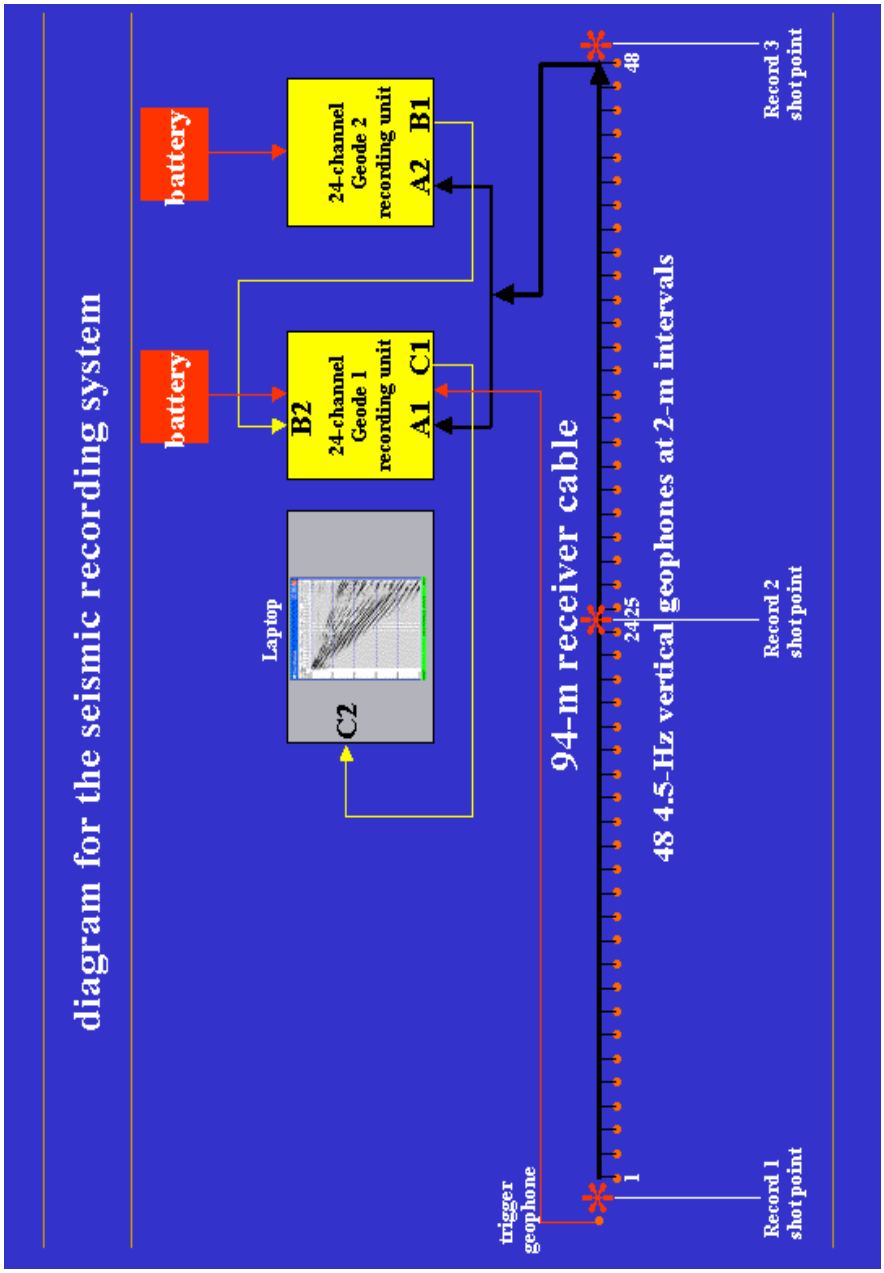

Figure 2.4 Workflow diagram of field survey in MASW

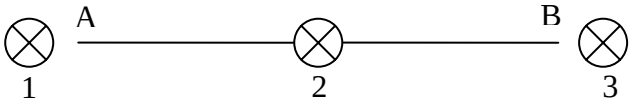

Figure 2.5 Site sketch for station: Line AB is 94 m-geophone spread, shot points 1 and 3 are located at 2 m horizontal offset from geophone spread and shot point 2 is located at the center of spread

2.3.2 Borehole Seismic Test

The borehole seismic test (BHS) is conducted on selected sites to determine V_s profiles by an alternative technique. An impact source located near the borehole is used. At any depth the travel time of the incident shear wave is recorded and shear wave velocity is calculated. The main difference between MASW and BHS is that the BHS provides V_s profiles at one point whereas MASW gives the laterally averaged V_s profile beneath the geophone spread. The lithology and borehole conditions affect the borehole results (Yılmaz et al., 2007). Case studies show that V_s profiles obtained by MASW and BHS can be 7 to 18% different (Park et al. 1999, Xia et al., 1999, 2002, and 2006). The agreement is better in alluvial deposits than in rocks that have large cavities (Yılmaz et al., 2008a).

The system of BHS was composed of mostly the same recording instruments but different configuration. Firstly a borehole was opened and cased with PVC. A 14-Hz geophone was lowered to a selected depth for recording the ground motion.

On the ground surface, 3 shots (i.e. impact source) were performed, one inducing vertical displacements for obtaining the V_p profile and two inducing horizontal displacements for obtaining V_s profile. For vertical shots a hammer was released to a plate to generate P-waves. In case of horizontal shots, a wooden block, located 1 m apart from the hole, was used to generate shear waves. As a checkpoint, the times of first arrival of shear waves should be identical for both horizontal shots (Yılmaz et al., 2008a).

A set of ground motion was recorded for each 1 m increment in depth until end of a borehole. A representative diagram is shown in Figure 2.6. From the received data, the first arrival times of primary and shear waves were selected. Then, first arrival times were corrected according to inclination of line between source and receiver (i.e., cosine correction). Afterwards, the variation of traveltime (t) with depth (z) ($\Delta t/\Delta z$) was computed, the layer boundaries were determined by marking depths where largest change in $\Delta t/\Delta z$ occurs, and V_s was calculated for each layer (Yılmaz et al., 2008a).

2.4 Results

A total of 153 NSMR-sites were investigated with SPT and MASW. Soil and rock descriptions were also presented for the upper 30 m of site. Moreover, the laboratory tests were employed for soil classification wherever applicable. An example summary report on site conditions, showing layer descriptions, SPT blow-counts and V_s profile, is presented in the Figure 2.7. The same type of information is available for all NSMR-sites. The classification of NSMR-sites according to seismic and geotechnical information is presented in the following chapter.

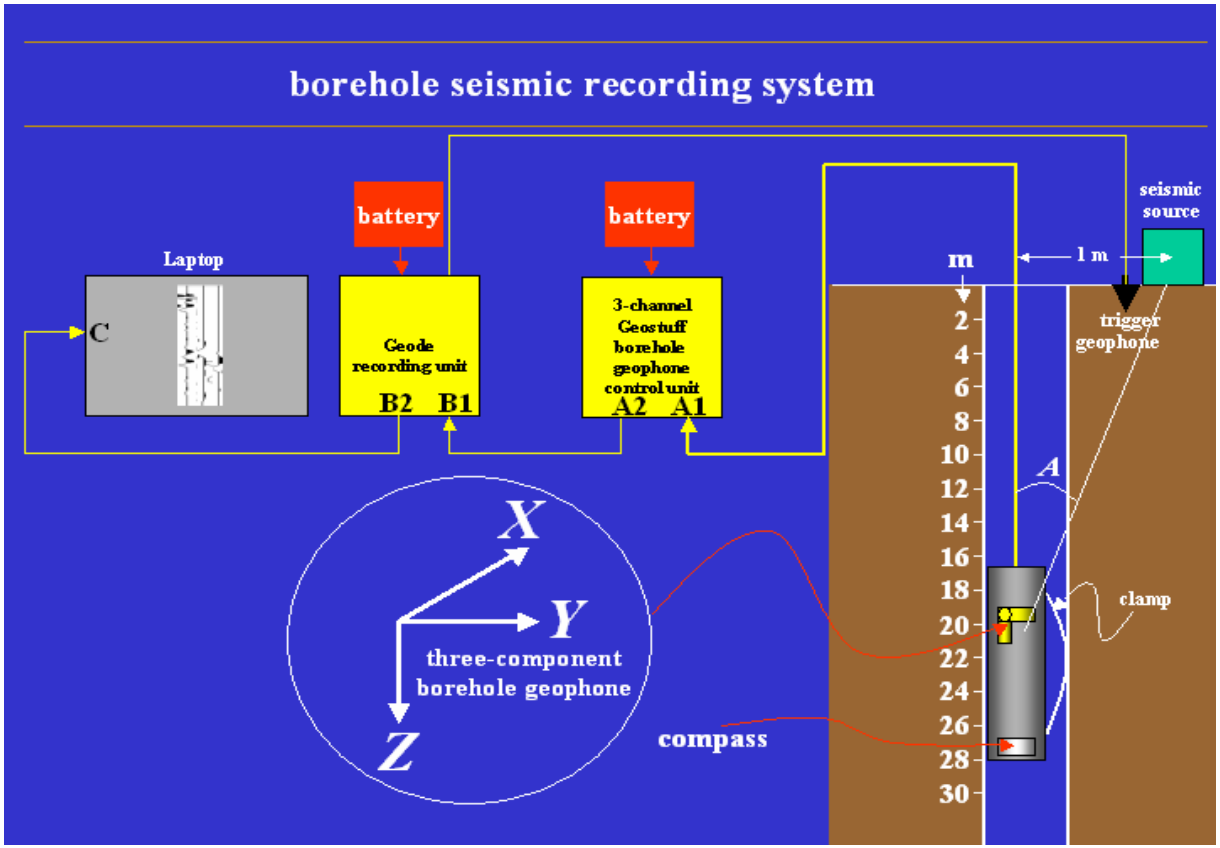

Figure 2.6 Workflow diagram of field survey in BHS

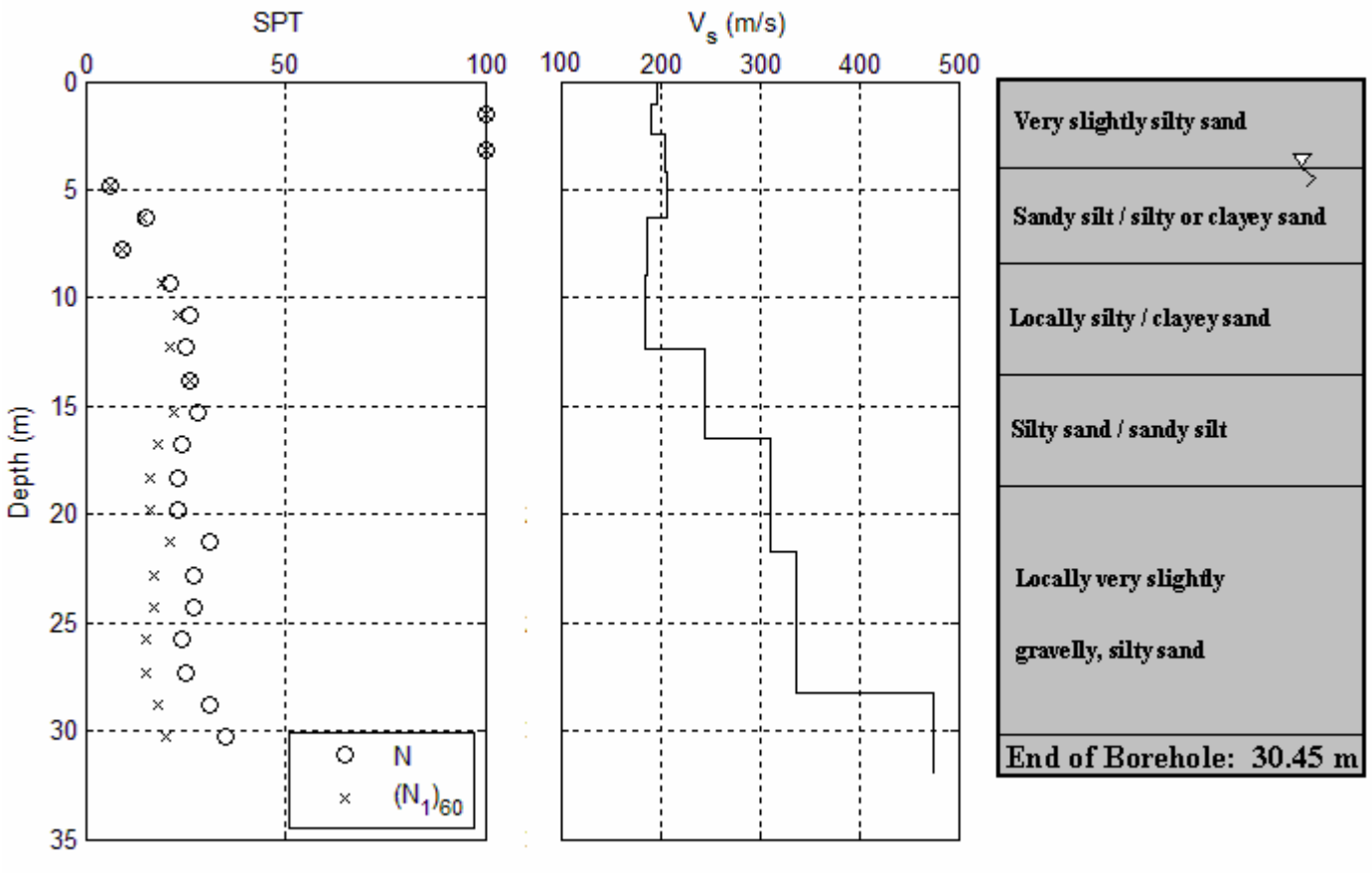

Figure 2.7 An example for summary report on site conditions

CHAPTER 3

SITE CLASSIFICATION OF NSMR SITES

3.1 Introduction

The site classifications for 153 NSMR-sites were carried out by employing the shear wave velocity profiles and SPT blow-counts obtained for the uppermost 30 m of soil/rock profile, with reference to NEHRP Provisions (BSSC, 2003), EC-8 (CEN, 2003) and TSDC (GDDA, 2007). Since TSDC has a very different site classification system from the others, the site classes according to NEHRP Provisions and EC-8, which are very similar, are primarily investigated, before the classification with TSDC.

The site classes are determined by application of shear wave velocity and penetration resistance criteria offered by the aforementioned codes. Since the number of unconfined compression tests is comparatively low and there is no continuous cohesive soil profile, the criterion for undrained shear strength (S_u) is not employed for site classification.

3.2 Site Classification According to NEHRP Provisions

NEHRP Provisions (BSSC, 2003) suggest a site classification system based on mean shear wave velocity ($V_{s,30}$), mean penetration resistance (N_{mean}) and mean undrained shear strength ($S_{u,30}$) of the uppermost 30 m. The site class definitions are presented in Table 3.1. In addition, NEHRP

Provisions propose class F sites requiring detailed site specific analysis. These are sites that contain profiles of at least 36 m thick medium stiff clays with S_u < 50 kPa and that have at least 3 m thickness of layers composed of highly organic clays or very plastic clays with PI > 75. However, no such conditions were encountered among the NSMR-sites. Finally, sites with potential of liquefaction also require site specific analyses. Accordingly, the NSMR-sites with soils susceptible to liquefaction were identified and presented in Chapter 4.

Table 3.1 Site class definitions in NEHRP Provisions (BSSC 2003)

Site Class	$V_{s,30}$ (m/s)	N_{mean}	$S_{u,30}$ (kPa)
A	$V_{s,30} > 1500$	-	-
B	$760 < V_{s,30} \leq 1500$	-	-
C	$360 < V_{s,30} \leq 760$	$N_{mean} > 50$	$S_{u,30} > 100$
D	$180 \leq V_{s,30} \leq 360$	$15 \leq N_{mean} \leq 50$	$50 \leq S_{u,30} \leq 100$
E	$180 \leq V_{s,30} \leq 360$	$15 \leq N_{mean} \leq 50$	$50 \leq S_{u,30} \leq 100$
	Any profile with more than 3 m of soft clay defined as soil with PI > 20, w ≥ 40% and S_u < 25 kPa		

The mean shear wave velocity of uppermost 30 m of site is calculated by

$$V_{s,30} = \frac{\sum_{i=1}^{i=n} d_i}{\sum_{i=1}^{i=n} \frac{d_i}{V_{si}}} \tag{3.1}$$

and the mean penetration resistance is calculated by

$$N_{mean} = \frac{\sum_{i=1}^{i=n} d_i}{\sum_{i=1}^{i=n} \frac{d_i}{N_i}} \tag{3.2}$$

where d_i is the thickness of i^{th} layer and V_{si} and N_i is the shear wave velocity and penetration resistance of the i^{th} layer, respectively.

The V_s profiles obtained from the MASW measurements were used to compute the $V_{s,30}$ for each site. Among 153 NSMR-sites, 85 are classified as class D, 65 are classified as class C, and the remaining 3 are classified as class B. Neither class A nor class E sites are available in the dataset. The NSMR-sites are also classified according to the N_{mean} of the uppermost 30 m soil profile. The numbers of sites classified according to the SPT criterion are 69, 76 and 8 for classes C, D, and E, respectively. The histogram of the site classes according to V_s and SPT criteria in NEHRP Provisions is given as Figure 3.1. The agreement of both criteria is investigated in detail in Section 3.4. The site class of each NSMR-site is given in Appendix A. The significance of correction of penetration resistance in site classification is presented in the following section.

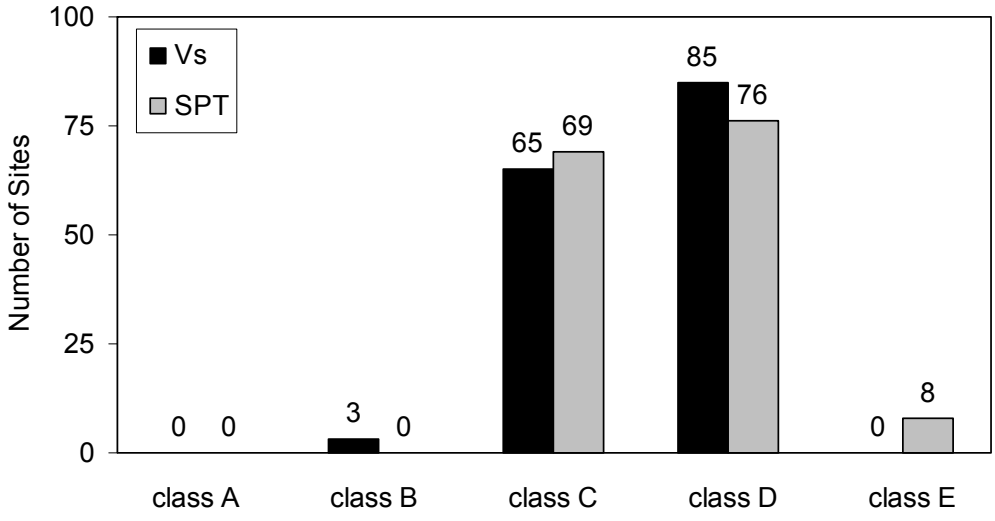

Figure 3.1 Histogram of the site classes according to NEHRP Provisions

3.3 Effect of the Penetration Resistance Correction on the Site Classification

Although no SPT correction is demanded before applying geotechnical criterion in NEHRP Provisions, the significance of SPT correction in site classification is critically evaluated. Two types of correction procedures are considered. The first is the correction for energy efficiency and the second is the implementation of complete SPT correction procedure as proposed by Youd et al. (2001). The complete procedure involves the energy correction as well.

The penetration resistance corrected for energy efficiency, N_{60} is calculated by multiplying N with the energy correction factor, C_E

$$N_{60} = N \times C_E \tag{3.3}$$

Energy correction factor arises due to differences between energy efficiencies of different hammer types. When safety hammer is used, the energy transferred to the rod is about 60% of the total potential energy of the hammer (Sivrikaya and Toğrol, 2006), and this percentage is widely accepted as a standard for energy efficiency of SPT (i.e. C_E=1). In the investigation of NSMR sites, SPT was performed by a donut hammer and two turns of rope on cathead. Thus, energy efficiency transferred to the rod is considered as 50% (Erdoğdu, 2007). Accordingly, C_E is taken as 0.83 in this study.

The completely corrected penetration resistance, $(N_1)_{60}$ is calculated by the procedure proposed by Youd et al. (2001). The procedure considers the effect of effective overburden pressure (C_N), energy efficiency of hammer (C_E), borehole diameter (C_B), rod length (C_R) and type of samplers (C_S) on N. $(N_1)_{60}$ is calculated by

$$(N_1)_{60} = C_N \times C_E \times C_B \times C_R \times C_S \times N \quad (3.4)$$

During the investigations, the sampler was used without liners. Therefore, C_S is assumed as 1.2 in this study. The borehole diameter was 10 cm which corresponds to C_B=1.0. C_E is taken as 0.83 as previously mentioned. Rod length correction factor is determined by length of the rod which is driven into ground and the C_R values are presented in Table 3.2.

Table 3.2 Rod length correction factors

Rod Length (m)	C_R
L < 3	0.75
3 ≤ L< 4	0.80
4 ≤ L< 6	0.85
6 ≤ L< 10	0.95
L ≥ 10	1.00

The total and effective vertical overburden stresses, σ_v and σ_v' must be predicted by employing the available information on soil profile. One of the advantages of SPT is to obtain disturbed samples that are used for soil classification by visual inspection and laboratory tests. Hence, soil class definitions and penetration resistances can be used to estimate the unit weight of soil layers. Some of the textbooks on soil mechanics and foundation engineering (e.g., Bowles (1996), Budhu (2000) and Das (2002)) were surveyed in order to estimate the wet and saturated unit weights of each soil type. The unit weight estimates for soils encountered in site investigations are listed in Table 3.3. The depth reached at the end of first 30 cm penetration of sampler during SPT was considered in calculation of

overburden pressure. σ_v is calculated by integrating unit weight of soil between ground surface and depth of SPT. In contrast, σ_v' is calculated by employing buoyant unit weight (i.e., saturated unit weight of soil minus unit weight of water) for soils beneath ground water level. The overburden pressure correction factor, C_N is applied only for sandy layers (Craig, 2002) and calculated by the formula

$$C_N = \sqrt{\frac{100}{\sigma'_v}} \tag{3.5}$$

where σ_v' is in kPa.

Table 3.3 Presumed unit weight of soils in overburden stress calculations

Soil Type	N Range	Wet Unit Weight (kN/m^3)	Saturated Unit Weight (kN/m^3)
very loose sand	0-4	13	15
loose sand	5-10	14	17
medium dense sand	11-30	17	19
dense sand	31-50	18	20
very dense sand	> 50	20	22
very loose gravel	0-4	14	17
loose gravel	5-10	15	18
medium dense gravel	11-30	18	20
dense gravel	31-50	19	22
very dense gravel	> 50	21	23
very soft silt	0-2	14	14
soft silt	3-4	15	15
medium stiff silt	5-8	17	17
stiff silt	9-15	18	18
very stiff silt	16-30	19	19
hard silt	> 30	20	20

Table 3.3 (Cont'd)

Soil Type	N Range	Wet Unit Weight (kN/m^3)	Saturated Unit Weight (kN/m^3)
very soft clay	0-2	15	15
soft clay	3-4	16	16
medium stiff clay	5-8	18	18
stiff clay	9-15	19	19
Very stiff clay	16-30	21	21
hard clay	> 30	22	22

In order to investigate the significance of SPT correction in the site classification, the term N in Equation 3.2 is replaced with N_{60} and $(N_1)_{60}$. Then, the mean penetration resistance with correction for energy efficiency, $(N_{mean})_{60}$ and mean penetration resistance with complete SPT correction, $(N_{mean})_{1,60}$ are calculated for each site. The differences between $(N_{mean})_{60}$ and N_{mean} are shown in Figure 3.2 as a function of N_{mean}. Similarly, the differences between $(N_{mean})_{1,60}$ and N_{mean} are illustrated in Figure 3.3.

It is expected that the energy correction may tend to give softer site classes because of the reduction in penetration resistances. As in Figure 3.2 the residuals are always less than zero except for a few sites that nearly all penetration tests resulted in refusals (N=100). The application of energy correction leads to reduction in N_{mean}. The most significant reduction is attained when N_{mean} is around 50. However, reduction becomes less significant as N_{mean} approaches to 100. The reason is that the tests refusals, which are accepted as N=100 without any correction, become more important as N_{mean} increases. There is no obvious trend in the difference between $(N_{mean})_{1,60}$ and N_{mean}, but generally $(N_{mean})_{1,60}$ is lower than N_{mean} with much scatter in the difference. Finally, the $(N_{mean})_{60}$ and

$(N_{mean})_{1,60}$ are contrasted in Figure 3.4. Generally, $(N_{mean})_{60}$ is a good approximator for $(N_{mean})_{1,60}$ with limited residuals.

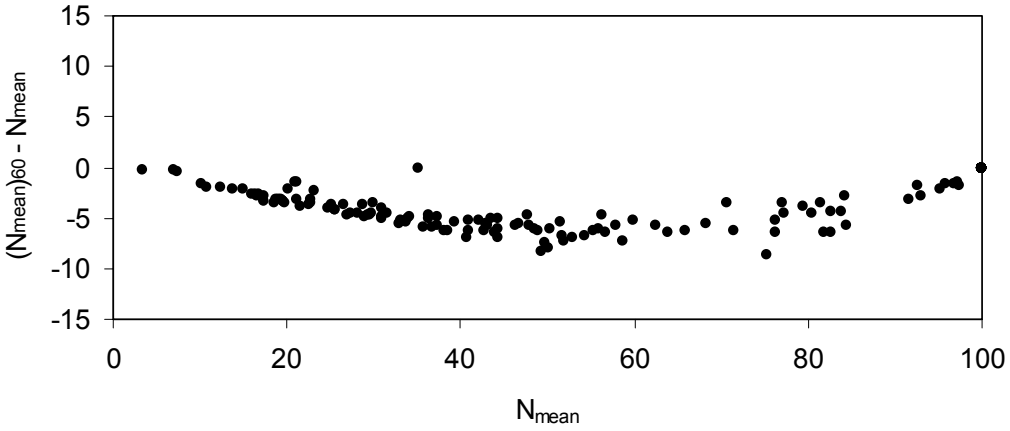

Figure 3.2 Comparison of $(N_{mean})_{60}$ with N_{mean}

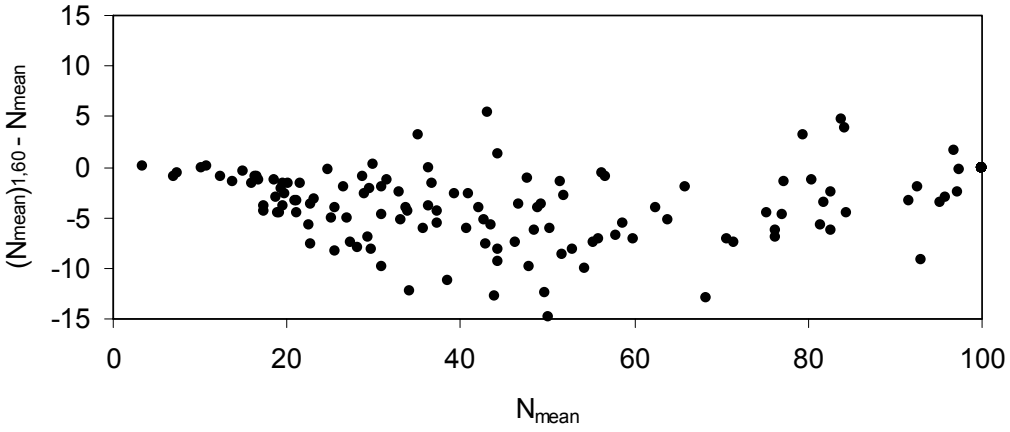

Figure 3.3 Comparison of $(N_{mean})_{1,60}$ with N_{mean}

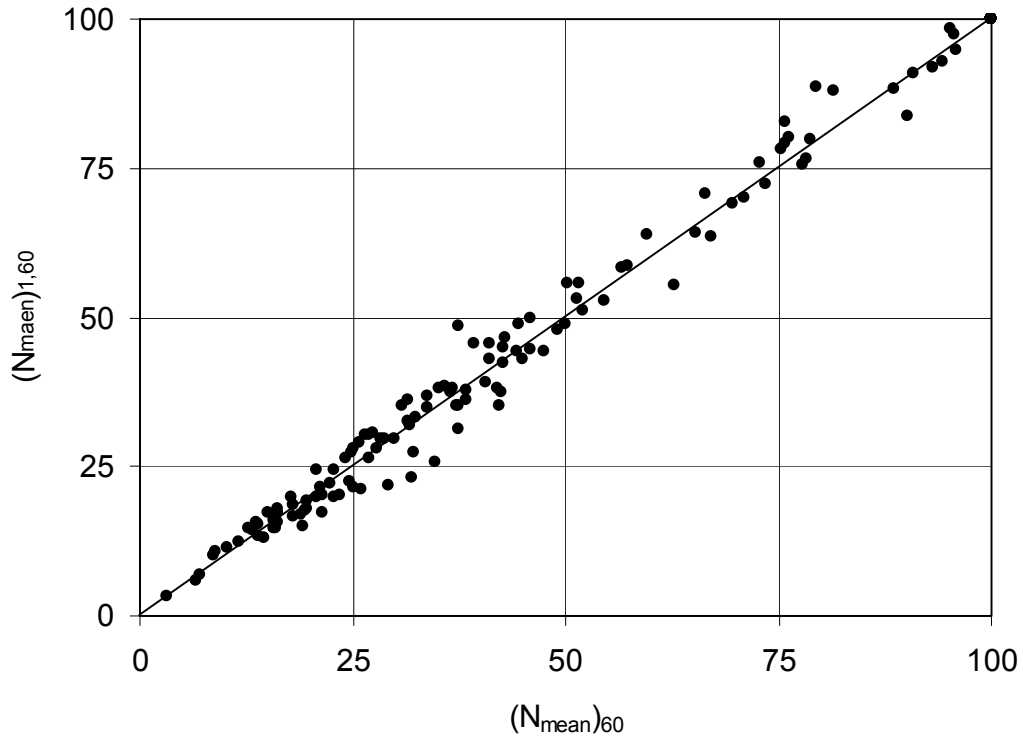

Figure 3.4 Comparison of $(N_{mean})_{60}$ and $(N_{mean})_{1,60}$

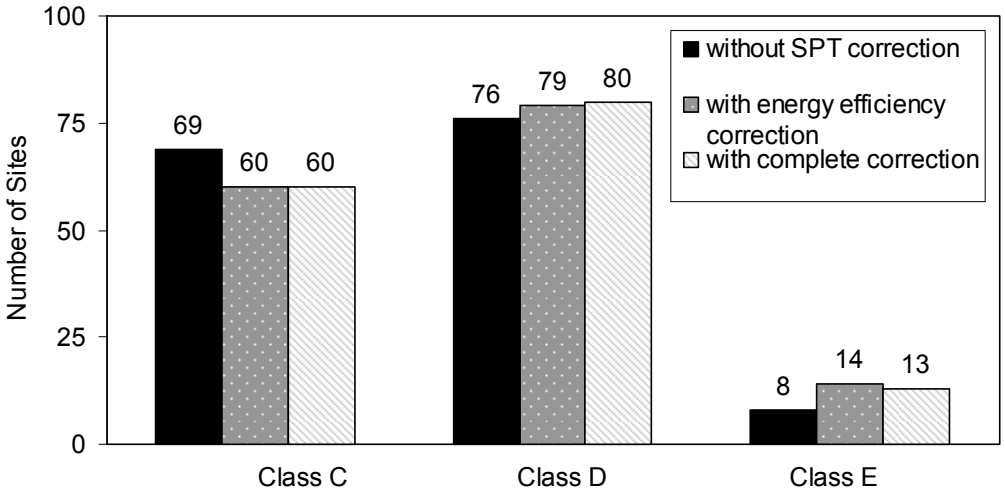

Figure 3.5 Comparison of site classes obtained without SPT correction, with energy efficiency correction, and with complete SPT correction procedure

The sites are re-classified using corrected penetration resistances. The histogram of site classes is illustrated in Figure 3.5. The correction effect on class D is negligible whereas the same conclusion can not be made for class C and E. Both corrections resulted in a similar increase in the number of softer site classes. Hence, correction for only energy efficiency (i.e., C_E) is sufficient, and complete correction of blow-counts appears to be rather unnecessary.

3.4 Consistency of Geotechnical and Seismic Criteria

The consistency between geotechnical and seismic criteria is important in engineering practice, since usually geotechnical information is available to engineers for foundation design. Considering NEHRP Provisions, consistency of geotechnical (i.e., N and N_{mean}) and seismic criteria (i.e., V_s and $V_{s,30}$) is critically evaluated in this section.

For further discussion, the term 'consistent' is used for sites for which seismic and geotechnical criteria result in the same site classes. Otherwise, the term 'inconsistent' is used. The seismic criterion is fundamental for site classification (Dobry et al., 2000). Therefore, the inconsistency is referred to as a safe one if geotechnical criterion provides a softer site class, because an engineer will employ higher spectral acceleration values in the mid- and long-period ranges of design spectrum. Otherwise, the inconsistency is referred to as an unsafe one. The comparisons of site classes obtained from $V_{s,30}$ and N_{mean}, $(N_{mean})_{60}$, and $(N_{mean})_{1,60}$ are presented in Figure 3.6.

Out of 153 NSMR-sites, the number of inconsistent but safe classification is 25, 35, and 34 when N_{mean}, $(N_{mean})_{60}$ and $(N_{mean})_{1,60}$ are used for geotechnical criterion respectively. On the other hand, the respective numbers are 15, 10, and 10 for unsafe classification. The proportion of unsafe classification is 9.8% (95% upper confidence limit, UCL, is 14.5%;

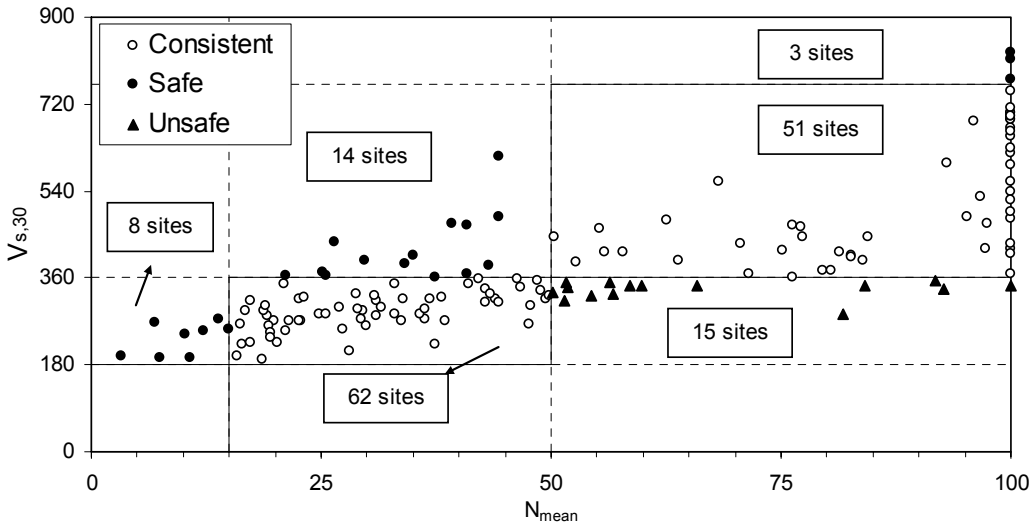

(a)

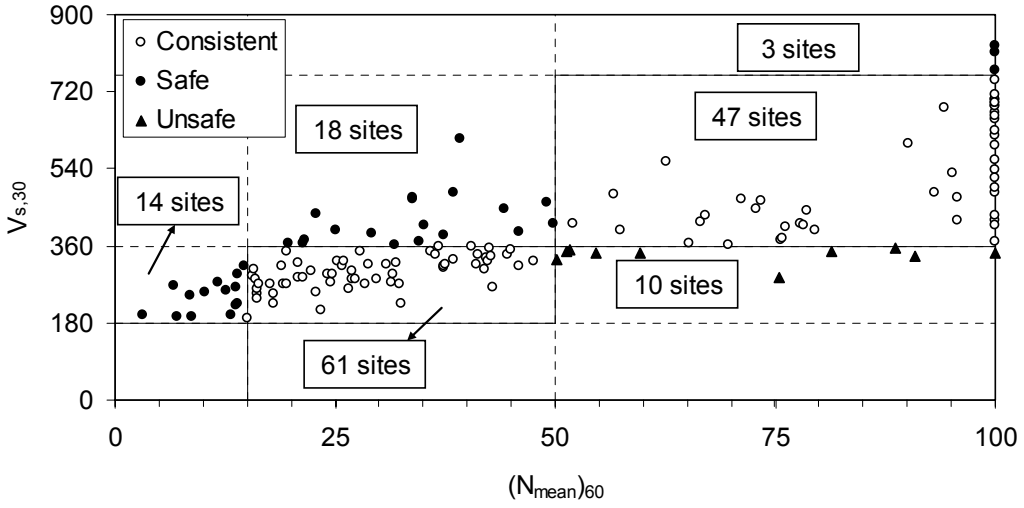

(b)

Figure 3.6 Comparison of site classes according to NEHRP Provisions (a) with no SPT correction (b) with correction for energy efficiency and (c) with complete SPT correction

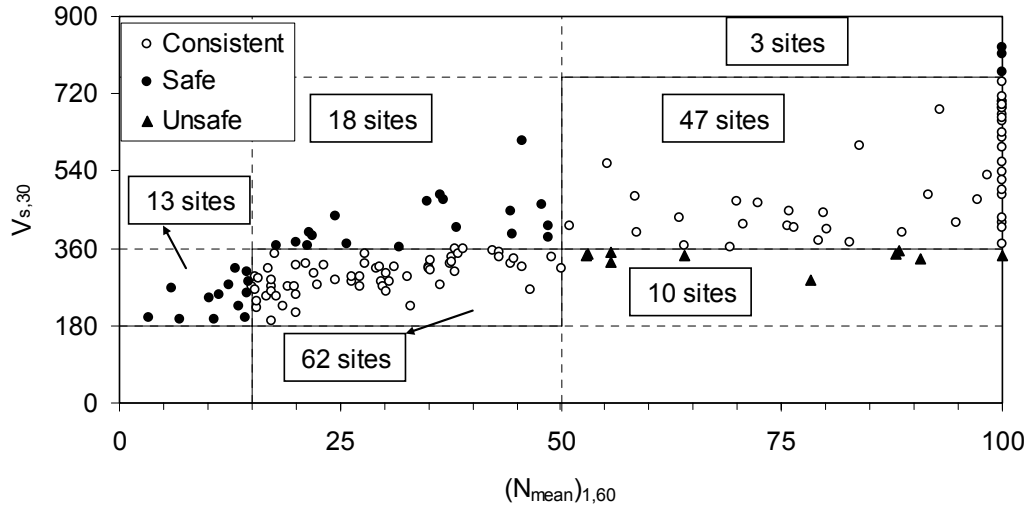

(c)

Figure 3.6 (Cont'd)

Devore, 2004) when N_{mean} is employed for site classification. However, the figures are 6.5% (95% UCL is 10.6%) when $(N_{mean})_{60}$ and $(N_{mean})_{1,60}$ are employed. Hence, there is no difference between employing parameters $(N_{mean})_{60}$ and $(N_{mean})_{1,60}$ in statistical perspective. Therefore, considering the relative ease of energy efficiency correction alone, use of $(N_{mean})_{60}$ instead of N_{mean} for site classification appears to provide safer results when geotechnical criterion is used.

When SPT is refused, N should be accepted as 100 according to NEHRP Provisions. 1105 SPT refusals were met in the site investigations, which were generally (70% of all refusals) met whenever V_s exceeds 360 m/s. 66 of these have V_s greater than 760 m/s. Hence, 64% of all refusals were met in layers that V_s is between 360 m/s and 760 m/s, which are the velocity bounds for site class C. This result confirms that geotechnical criterion can

not be used for site classes A or B, as stated by NEHRP Provisions. Moreover, the gravelly layers show generally SPT refusals (58%), whereas only 72% of these refusals are obtained when V_s is greater than 360 m/s. SPT predicts stiffer conditions than those predicted by seismic tests for 26% of all SPT tests in gravels layers. Hence, geotechnical criterion (SPT) is apparently less reliable for classification of sites with thick gravelly layer, due to inappropriateness of split-spoon sampler in gravelly soils.

The scattering of V_s with N and N_{60} is shown in Figure 3.7. The data that involves SPT refusals, and that is obtained from gravel layers is omitted. The consistency of SPT results with V_s according to bounds given in Table 3.1 is investigated, considering each test result instead of the mean value for each site. In case N is used, the proportion of consistent (N, V_s) data pairs is 52% (95% confidence interval, CI is [%49, %54]) and 95% UCL of unsafe inconsistency is 12.7%. In case N_{60} is employed, the proportion of consistent data pairs is 47% (95% CI is [%44, %50] and 95% UCL of unsafe results is 8.4%.

Additionally, the effect of homogeneity of soil profile on consistency between results of SPT and MASW is investigated. Only the data from homogeneous soil layers is used. A layer is considered as homogeneous in case V_s determined by MASW method is constant between presumed layer boundaries, and soil specimens (sample size is at least 3) show similar particle sizes. The scatter plot for V_s versus N is given as Figure 3.8. The proportion of consistent data pairs is 58% (%95 CI is [%55, %60]) and 95% UCL of unsafe results for SPT is 18.4%. In case N_{60} is used, the proportion of consistent data pairs is 55% (95% CI is [%52, %58]) and 95% UCL of unsafe soil classification is 15.3%.

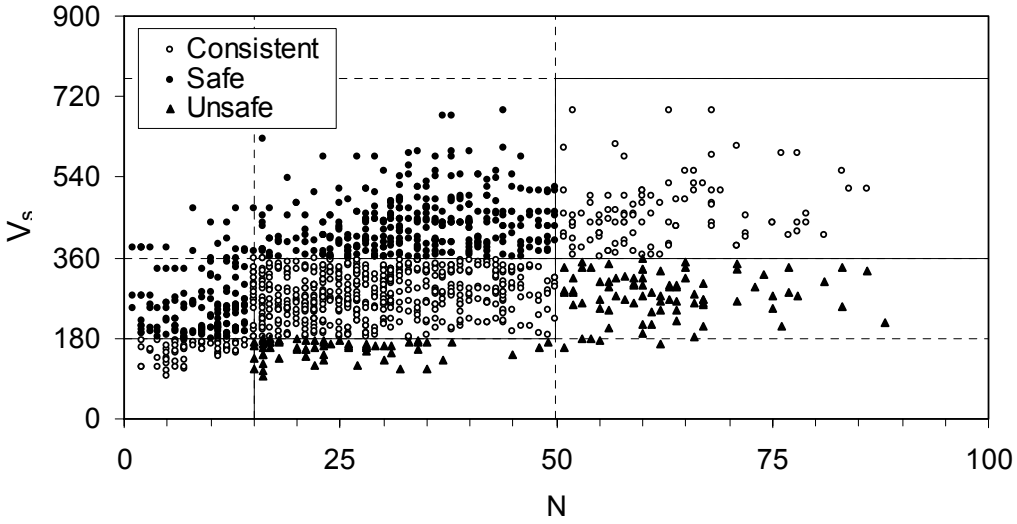

(a)

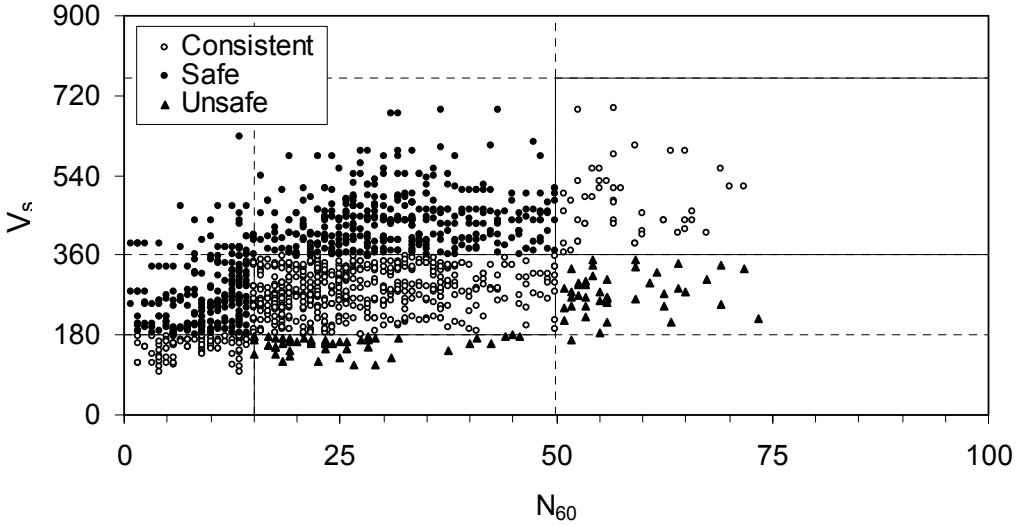

(b)

Figure 3.7 The compatibility of N with V_s (a) with no SPT correction and (b) with energy efficiency correction

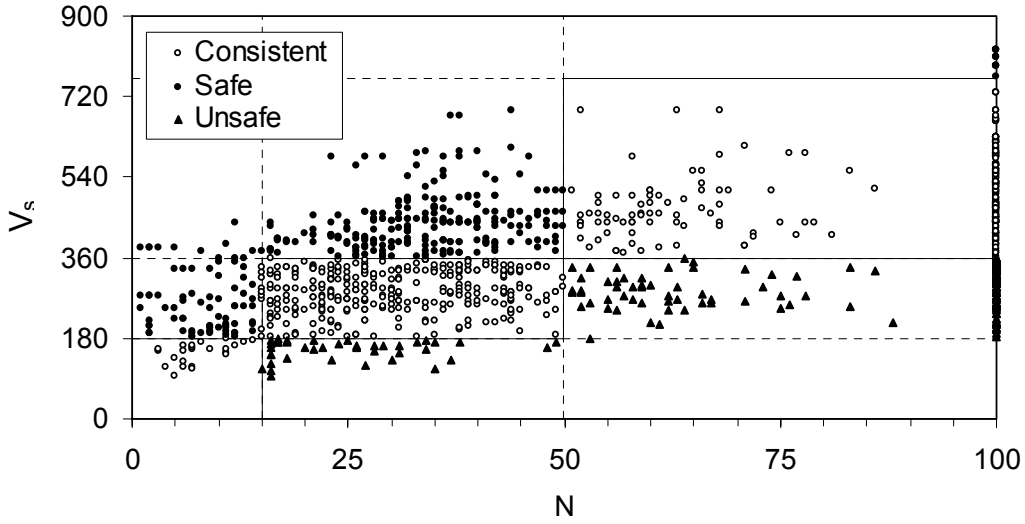

(a)

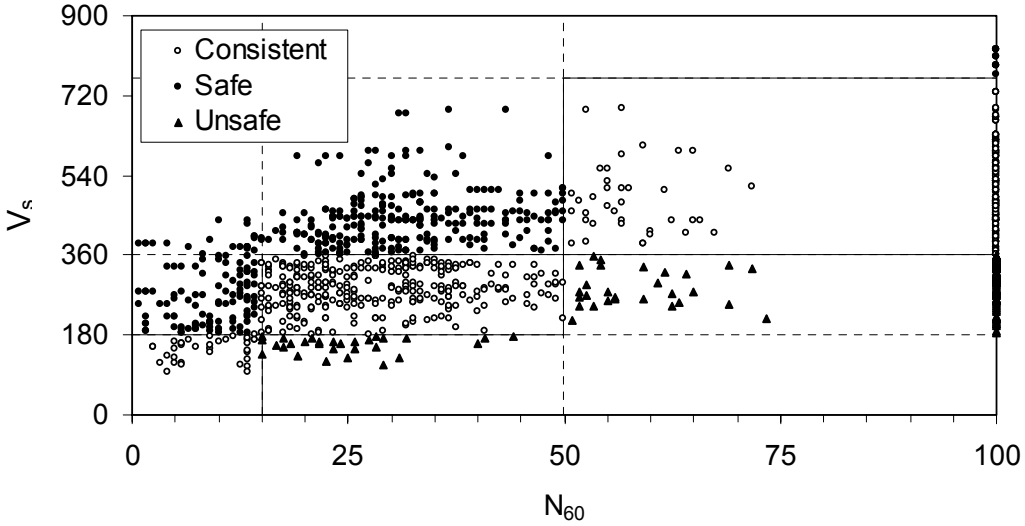

(b)

Figure 3.8 Comparison of data that homogeneity of layers is satisfied (a) with no SPT correction and (b) with energy efficiency correction

Hence discrepancy between results of SPT and MASW can not be explained by the vertical heterogeneity of soil profiles. However, the use of N_{60} instead of N slightly reduces proportion of unsafe classification by geotechnical criterion.

3.5 Site Classification According to EC-8

EC-8 (CEN, 2003) suggests a site classification scheme similar to NEHRP Provisions. The site class definitions are shown in Table 3.4. Excluding the sites that require site specific analysis, the geotechnical criteria of two codes are the same. On the other hand, the definitions of the sites which require site specific analysis are different. There is not any class S1 site in the dataset. In addition, class S2 is related to soil liquefaction and not considered in this section.

Table 3.4 Site class definitions in EC-8 (CEN 2003)

Site Class	$V_{s,30}$ (m/s)	N_{mean}	$S_{u,30}$ (kPa)
A	$V_{s,30} > 800$	-	-
B	$360 < V_{s,30} \leq 800$	$N_{mean} > 50$	$S_{u,30} > 250$
C	$180 \leq V_{s,30} \leq 360$	$15 \leq N_{mean} \leq 50$	$70 \leq S_{u,30} \leq 250$
D	$V_{s,30} < 180$	$N_{mean} < 15$	$S_{u,30} < 70$
E	A soil profile consisting of a surface alluvium layer with V_s in the range given for sites of type C or D, with thickness varying between 5 m and 20 m and which is underlain by stiffer material with $V_s > 800$ m/s		
S1	Deposits containing a layer of soft clays/silts with a high plasticity index (PI > 40) and high water content with $V_s < 100$ m/s or $10 < S_u < 20$ kPa, and at least 10 m thick		
S2	Deposits of liquefiable soils, of sensitive clays, or any other soil profile not included in types A – E or S1		

One of the two basic differences between the seismic criteria in EC-8 and NEHRP Provisions is that class A and class B of NEHRP Provisions are integrated in EC-8 as class A. The class A-B boundary of EC-8 is increased to 800 m/s whereas the corresponding boundary in NEHRP Provisions is 760 m/s. This leads to virtually the same site classes for EC-8 and NEHRP Provisions: Classes D, C and B in EC-8 correspond to classes E, D and C in NEHRP Provisions, respectively. However, there is only one site (AI_114_GZL) that has different site classes when seismic criterion is used.

The other difference is that EC-8 includes a different site class, class E that is related with soft deposits underlain by very stiff deposits. However the database does not include this type of site. The histogram of the site classification obtained utilizing the V_s and SPT criterion of EC-8 are plotted in Figure 3.9. The site classes of all NSMR-sites according to EC-8 are tabulated in the Appendix A.

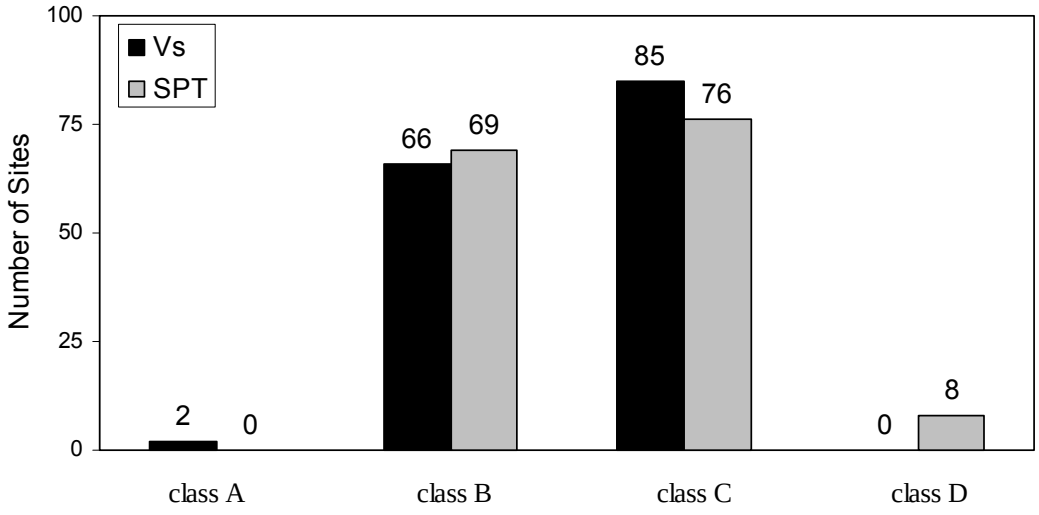

Figure 3.9 Histogram of the site classes according to EC-8

The difference of V_s limit for rock sites in EC-8 leads one more consistent site (AI_114_GZL) according to seismic and geotechnical criteria. Both NEHRP provisions and EC-8 give the same number of unsafely classified sites according to geotechnical criterion. Thus, the same conclusions with those given for NEHRP Provisions can be stated for EC-8.

3.6 Site Classification According to TSDC

Within the scope of the study, the NSMR-sites are also classified according to TSDC (GDDA, 2007). TSDC has a very different classification system from NEHRP Provisions and EC-8. The site class is determined by using the thickness of shallow soil or rocks, which are categorized according to lithological descriptions and measured values for V_s, N or q_u. These categories are referred to as subclasses.

Site classification in TSDC was first published in 1975 and no modifications were made in either 1997 or 2007 editions. Since TSDC proposed a site classification scheme primarily based on the shallow lithology, the layers should be first classified either as rock, coarse grained soil (sand and gravel) or fine grained soil (clay and silt). Then, the soil layers are categorized into subclasses according to V_s or N. The lithological, geotechnical and seismic descriptions for subclasses are given in Table 3.5. By using topmost subclass and its thickness, which should be at least 3 m, a site is classified according to the definitions given in Table 3.6.

The principles behind the site class definitions in TSDC are not explained in any widely accessible scientific paper. It is apparent that the classification is based on the assumption that the layers become stiffer by increasing depth. However, in many NSMR-sites, a contradictory situation to this assumption was met. Therefore, in order to classify the sites consistently, especially in the case of rather heterogeneous profiles, it is necessarily to establish

some additional rules. The sites are classified according to three steps that are given below.

Table 3.5 Subclass definitions in TSDC (GDDA 2007)

Subclass	Shallow lithology	N	V_s (m/s)	q_u (kPa)
(A)	Rock group 1	-	>1000	> 1000
	Very dense sand, gravel, etc.	> 50	> 700	-
	Hard clay, silty clay, etc.	> 32	> 700	> 400
(B)	Rock group 2	-	700 - 1000	500 - 1000
	Dense sand, gravel, etc.	30 - 50	400 - 700	-
	Very stiff clay, silty clay, etc.	16 - 32	300 - 700	200 - 400
(C)	Rock group 3	-	400 -700	< 500
	Medium dense sand, gravel, etc.	10 - 30	200 - 400	-
	Stiff clay, silty clay, etc.	8 - 16	200 - 300	100 - 200
(D)	Soft deep alluvial layers with high water table	-	< 200	-
	Loose sand, gravel, etc.	< 10	< 200	-
	Soft clay, silty clay, etc.	< 8	< 200	< 100

Rock Group 1: Massive volcanic rocks, unweathered sound metamorphic rocks, stiff cemented sedimentary rocks

Rock Group 2: Soft volcanic rocks such as tuff and agglomerate, weathered cemented sedimentary rocks with planes of discontinuity

Rock Group 3: Highly weathered soft metamorphic rocks and cemented sedimentary rocks with planes of discontinuity

Table 3.6 Local site class definitions in TSDC (GDDA 2007)

Local Site Class	Soil Subclass Definitions (h_1: topmost layer thickness)
Z1	Subclass (A) soils Subclass (B) soils with $h_1 \leq 15$ m
Z2	Subclass (B) soils with $h_1 > 15$ m Subclass (C) soils with $h_1 \leq 15$ m
Z3	Subclass (C) soils with 15 m $< h_1 \leq 50$ m Subclass (D) soils with $h_1 \leq 10$ m
Z4	Subclass (C) soils with $h_1 > 50$ m Subclass (D) soils with $h_1 > 10$ m

1. If a stiffer subclass with at least 3 m thickness is beneath a softer subclass with at least 3 m thickness, the softer subclass is used for site classification, as stated by TSDC.

2. If there is a softer subclass with at least 3 m thickness beneath a stiffer subclass, the stiffer subclass is disregarded and the softer subclass is used for site classification.

3. If the thickness of the softest subclass is less than 3 m, it is omitted in classification. In case that total thickness of the softest subclass is equal to or greater than 3 m in a very heterogeneous soil profile, it is used for site classification by considering its total thickness.

153 sites are classified according to seismic criterion whereas 94 of the sites can be classified according to geotechnical criterion. The sites that have rock formations and on which SPT is generally refused in layers with frequent boulders can not be classified. The histograms of site classes

according to the seismic and geotechnical criteria given by TSDC are presented in Figure 3.10. The site classes according to TSDC are also given in Appendix A.

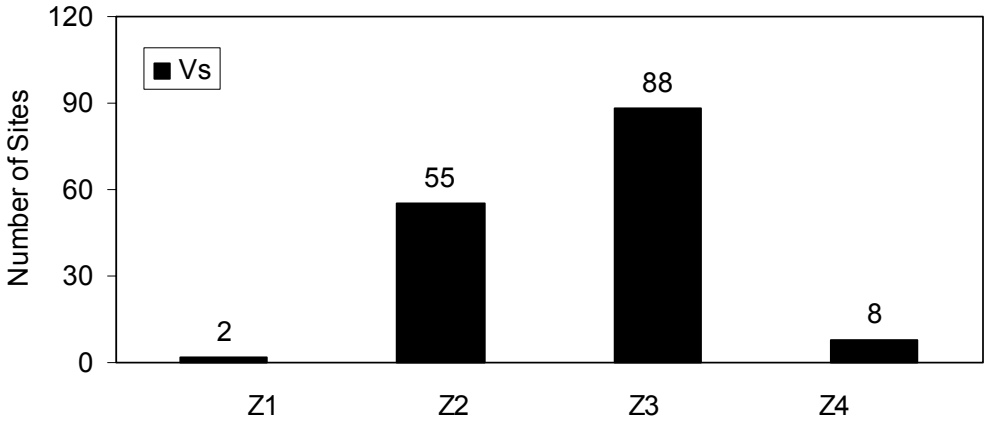

(a)

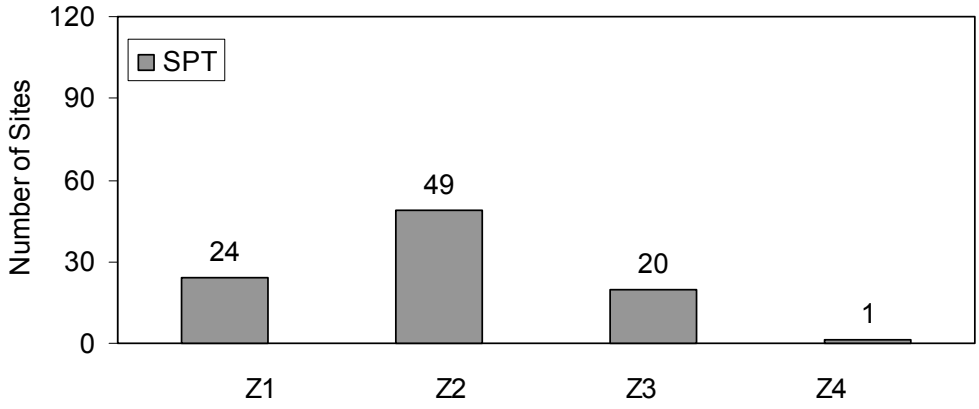

(b)

Figure 3.10 Histogram of the site classes according to TSDC (a) seismic criterion and (b) geotechnical criterion

The consistency between the geotechnical and seismic criteria in TSDC is also investigated as done considering the criteria in NEHRP Provisions. The histograms of classes of the 94 sites according to the seismic (V_s) and geotechnical (SPT) criteria are shown in Table 3.7. 21% of 94 sites (95% CI is [14%, 30%]) have consistent site classes according to the two criteria, and geotechnical criterion results in unsafe classification with respect to the seismic criterion for 62% (95% UCL is %70) of the sites.

Table 3.7 Comparison of site classes according to TSDC

		SPT criterion			
		Z1	Z2	Z3	Z4
V_s criterion	Z1	0	0	0	0
	Z2	10	15	1	0
	Z3	14	31	14	1
	Z4	0	3	5	0

The significant inconsistency between the site classes in TSDC is observed when V_s and N criteria are used separately. It is noted that this is not observed in either NEHRP Provisions or EC-8. It is clear that the geotechnical criterion in TSDC provides stiffer site classes. Consequently, geotechnical (SPT) criterion can generally lead to unsafe site classification, such that a lower spectral acceleration than what is necessary may be employed for design of a mid- or high-period structure. On the other hand, SPT criterion in other codes resulted in relatively less unsafe site classification.

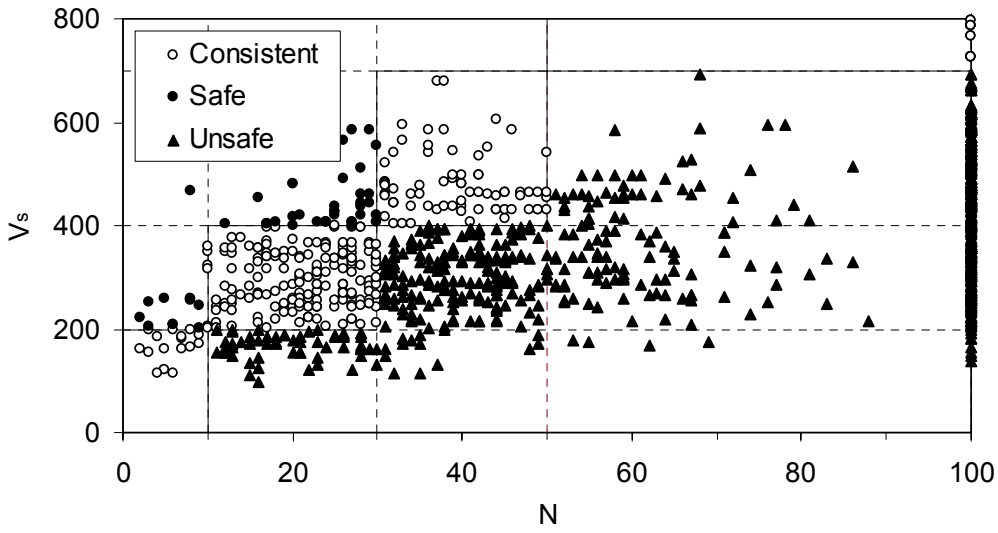

(a)

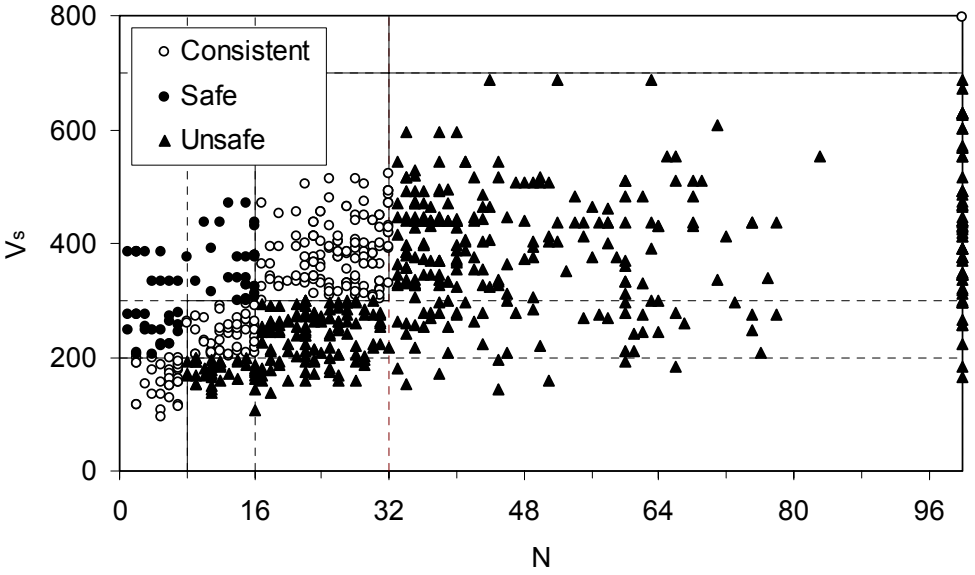

(b)

Figure 3.11 Consistency of SPT (N) with V_s for (a) coarse-grained soils, and (b) fine-grained soils

Considering SPT results performed at various depths, the scattering of V_s with N for coarse-grained and fine-grained soils is presented in Figures 3.11.a-b. The figures confirm that SPT bounds are not very consistent with V_s bounds given for site classes in TSDC.

In order to investigate the consistency between site classification systems given in NEHRP Provisions (hence, EC-8) and TSDC, the NSMR-site classes according to seismic criteria are compared in Table 3.8. It is observed that NEHRP class C sites are generally defined as Z2 and Z3 sites in TSDC. However Z3 sites are mostly classified as D according to NEHRP Provisions. However, considering the dispersion in results, it is concluded that there is no definite site-class counterparts in NEHRP Provisions to site classes in TSDC.

Table 3.8 Comparison of the site classes according to NEHRP Provisions and TSDC

		TSDC			
		Z1	Z2	Z3	Z4
NEHRP Provisions	B	0	3	0	0
	C	2	38	25	0
	D	0	14	63	8

CHAPTER 4

LIQUEFACTION ANALYSIS OF NSMR-SITES

4.1 Introduction

One of the most critical phenomena in the geotechnical earthquake engineering is liquefaction of cohesionless soils. Under cyclic loading, pore pressures in saturated soils can significantly increase, reducing the effective stresses. Consequently, a reduction in the shear strength of cohesionless soil occurs. When the excess pore pressure is almost equal to confining pressure, the effective stresses and shear strength of cohesionless soil is reduced to very small values (practically zero), and the material behaves rather as a liquid. This phenomenon is called liquefaction.

The site classes defined in NEHRP and EC-8 involve special classes for sites that require specific analysis. Liquefiable sites are among such sites. Since the ground motion characteristics can be strongly affected by liquefaction (Kramer, 1996, and Bakır et al., 2005). The assessment of possibility of liquefaction on NSMR-sites is necessary for studies that employ strong motion records obtained at these sites.

Assessment of liquefaction potential of a site is composed of two important steps: susceptibility and opportunity analysis (Yılmaz, 1999). The liquefaction susceptibility is the capability of the soil layer to resist liquefaction. The liquefaction opportunity can be defined as the seismic

demand on soil to initiate soil liquefaction. A site will have liquefaction potential if the seismic demand (i.e., opportunity) exceeds soil's capacity (i.e., susceptibility).

The liquefaction susceptibility can be determined from historical, geologic, and geotechnical criteria (Kramer, 1996). The liquefaction opportunity for future events can be usually determined from seismic hazard analysis. There exist numerous procedures available in the literature to evaluate the liquefaction potential. In practice, a well known simplified procedure was first introduced by Seed and Idriss (1971). Afterwards this study was improved by Seed (1979), Seed and Idriss (1982) and Seed et al. (1985), such that basic steps of analysis were formulated and the liquefaction resistance was related to the penetration resistance in sands. The most recent form of the simplified procedure was presented by Youd et al. (2001). The simplified procedure employs geotechnical data of cohesionless soils in order to estimate its liquefaction susceptibility either through utilization of simple charts (Figure 4.1) or relevant equations.

4.2 Liquefaction Susceptibility

The first prerequisite of liquefaction susceptibility is that the soil must be saturated (Kramer, 1996); the second, the type of deposit must be granular (i.e., can be practically compacted under cyclic shear stresses). Layers of sand that conform to these two conditions are investigated for susceptibility analysis. The case histories, which were used for the development of simplified procedure, involve data from shallow depths (<15 m), limiting the applicability of procedure to shallow layers. Hence, in this study, the layers below 15 m depth are not investigated.

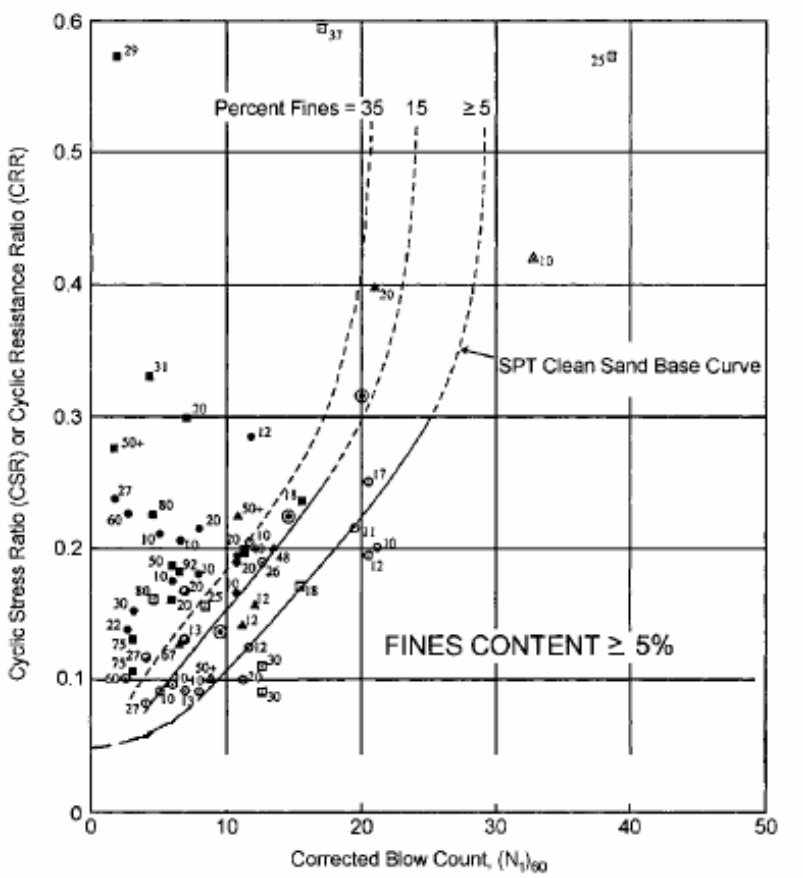

Figure 4.1 Case history data (Youd et al. 2001)

The conducted in-situ and laboratory measurements from 153 NSMR-sites provide necessary geotechnical parameters such as ground water level (GWL), penetration resistance (N), USCS descriptions of soils and fines content to evaluate the liquefaction susceptibility.

The resistance of saturated clean sand to liquefaction depends on $(N_1)_{60}$ (see Chapter 3). When a significant quantity of fine material is found in sand, a correction for fines content, FC, is applied to $(N_1)_{60}$ in order to

employ relationships given for penetration resistance in clean sands, $(N_1)_{60cs}$, such that

$$(N_1)_{60cs} = \alpha + \beta \times (N_1)_{60} \quad (4.1)$$

where α and β are the coefficients factors depending on FC. These coefficients can be determined by the equations provided in Table 4.1 (Youd et al., 2001).

Table 4.1 α and β equations for clean sand correction

	α	β
FC ≤ 5	0.0	1.0
5 < FC < 35	$\exp[1.76-(190/(FC)^2]$	$[0.99+(FC^{1.5}/1000]$
FC ≥ 35	5.0	1.2

In the simplified procedure, cyclic resistance ratio (CRR) is calculated for an earthquake of moment magnitude, Mw, 7.5 considering $(N_1)_{60cs}$:

$$CRR = \frac{1}{34 - (N_1)_{60cs}} + \frac{(N_1)_{60cs}}{135} + \frac{50}{[10 \times (N_1)_{60cs} + 45]^2} - \frac{1}{200} \quad (4.2)$$

Equation 4.2 fits to the clean sand curve given in Figure 4.1, and is valid only for the values of $(N_1)_{60cs}$ is less than 30. If $(N_1)_{60cs}$ is greater than 30, saturated sand can be accepted as a non-liquefiable material.

4.3 Liquefaction Opportunity

The liquefaction opportunity is generally expressed by intensity of ground motion. Whereas the peak ground velocity is applicable as a parameter, the simplified procedure uses peak horizontal acceleration (Orense, 2005, and Youd et al., 2001). Ground motion intensities can be found from ground motion prediction equations, site response analysis or seismic hazard maps.

The simplified procedure suggests the use of cyclic stress ratio (CSR) to express the seismic demand on soil. For an event of moment magnitude (M_w) 7.5, CSR is calculated by

$$CSR = 0.65 \times \left(\frac{a_{max}}{g}\right) \times \left(\frac{\sigma_v}{\sigma_v'}\right) \times r_d \qquad (4.3)$$

where a_{max} is peak horizontal acceleration at ground surface generated by the earthquake, g is the gravitational acceleration. σ_v and σ_v' are the total and effective vertical overburden stresses that are calculated as stated in the Chapter 3, respectively. r_d is the stress reduction factor which is a function of depth below ground surface (z)

$$r_d = \frac{1.0 - 0.4113 \times z^{0.5} + 0.04052 \times z + 0.001753 \times z^{1.5}}{1.0 - 0.4177 \times z^{0.5} + 0.05729 \times z + 0.006205 \times z^{1.5} + 0.00121 \times z^{2.0}} \qquad (4.4)$$

A correction factor is introduced for magnitudes different from 7.5, as stated in the following.

4.4 Liquefaction Potential

According to simplified procedure, which assumes free-field conditions, a site will have liquefaction potential if CSR>CRR. Generally, a safety factor is introduced in liquefaction potential assessment. In this study, the calculations are performed in order to determine the possibility of liquefaction for future events during which prospective ground motions will be recorded at NSMR-sites. Therefore, none of the aforementioned methods to estimate the a_{max} is employed. Hence, the liquefaction susceptibility of the sites is expressed in terms of peak horizontal ground acceleration necessary to trigger liquefaction. The term a_{max} in equation 4.3 is replaced with critical peak ground acceleration, a_{crt}, necessary for triggering of liquefaction. a_{crt} is calculated assuming that CSR=CRR for M_w=7.5. A site will have liquefaction potential if recorded peak horizontal ground acceleration is larger than a_{crt}.

4.5 Results

The layer where lowest a_{crt} is calculated is assumed as critical layer. Total of 31 sites were identified to consist of soils susceptible to liquefaction. The names of these sites, depth and total thickness of critical layers, and a_{crt} (for M_w=7.5) are listed in Appendix B. The histogram of a_{crt} for sites with soils susceptible to liquefaction is given as Figure 4.2.

For moment magnitudes different from 7.5, a_{crt} can be scaled by magnitude scaling factor, MSF, (Youd et al., 2001):

$$MSF = \left(\frac{M_w}{7.5}\right)^{-3.3} \tag{4.5}$$

The ground water levels (GWL) are influenced by climatic circumstances and the human activities. These cause variability in GWL, inspected in boreholes during drilling. The influence of GWL variability on liquefaction is analyzed. The GWL is sequentially increased by 1.0 m and histograms of a_{crt} for shallow GWL are given in Figure 4.3. The resistance of sites to liquefaction decreases as GWL gets shallower, since shallow sands generally have low penetration resistance and become susceptible to liquefaction when they are saturated. These results point out a limitation of the data and the analysis procedure presented in this chapter. Improved results that consider variability in GWL can be provided if the variations are monitored for several seasons.

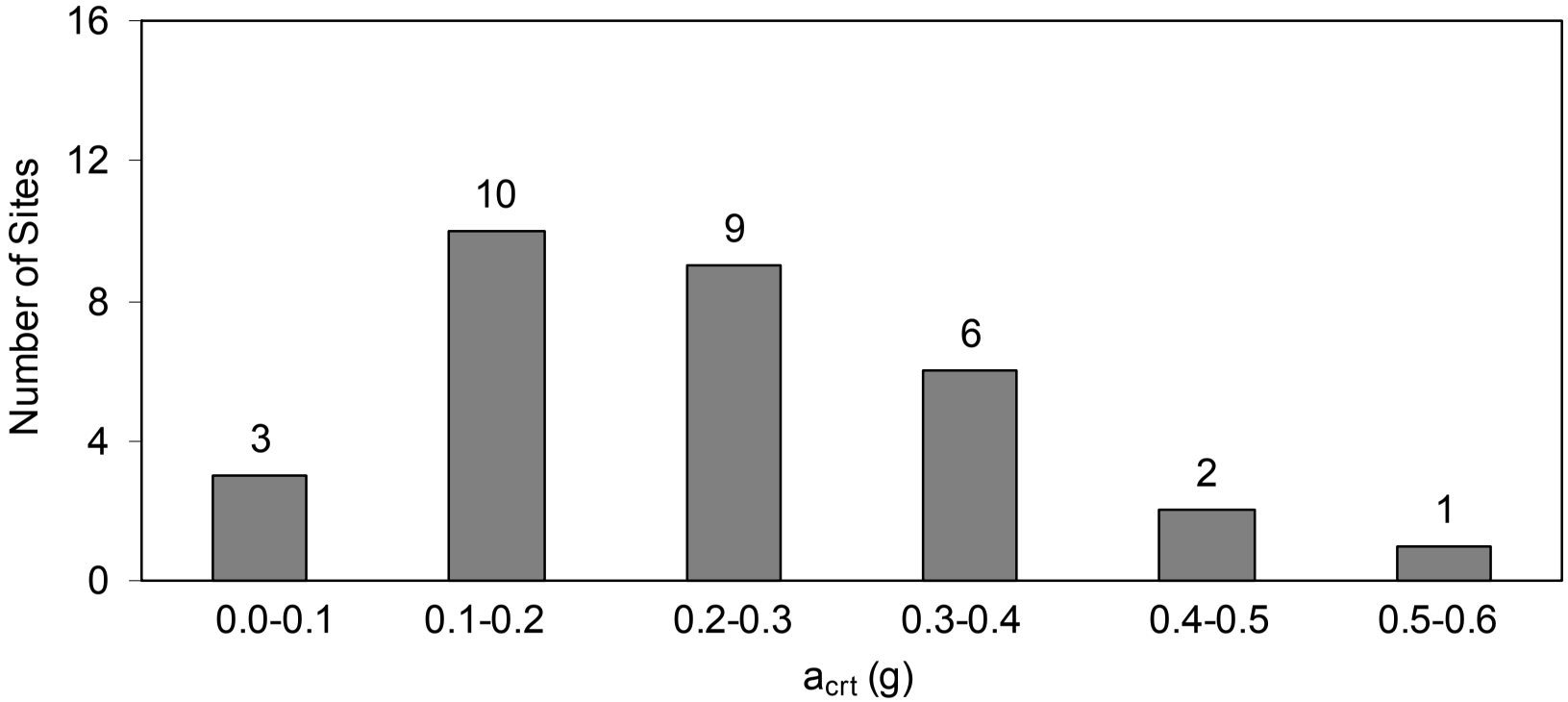

Figure 4.2 Histogram of a_{crt} on sites susceptible to liquefaction.

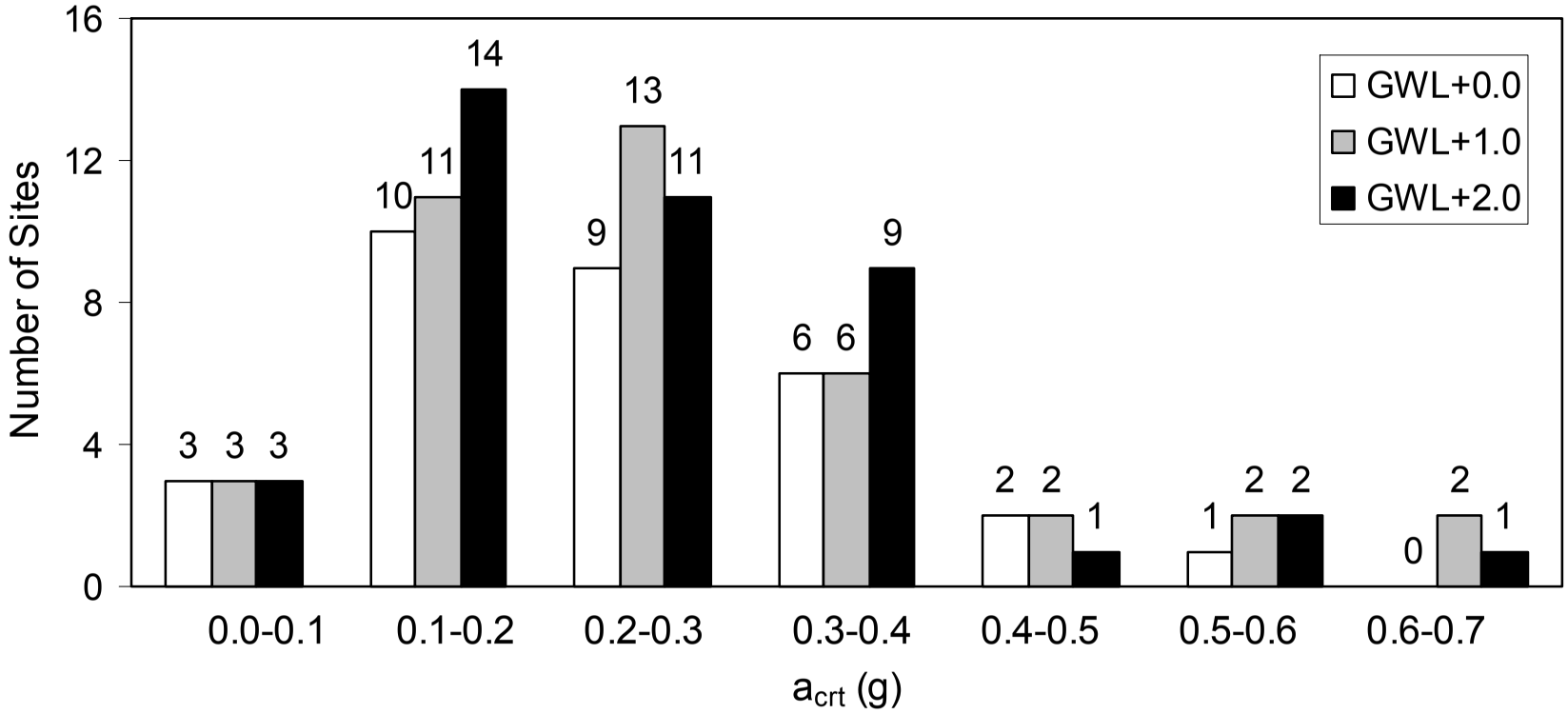

Figure 4.3 Histograms of a_{crt} on sites susceptible to liquefaction considering shallower GWL

CHAPTER 5

COMPARISON OF MASW WITH SASW AND BHS

Within the scope of the NSMP, V_s profiles were determined by (MASW) method at 153 sites. In addition, nine of these sites were selected for seismic survey by employing borehole seismic test (BHS). In this chapter, the comparisons of both tests are presented. The selected sites and the distances between the boreholes for BHS test and the centers of seismic lines for MASW method, and depth of explorations are presented in Table 5.1. Moreover, 6 of 153 sites, presented in Table 5.2 have V_s profiles obtained from SASW method applied by Rosenblad et al. (2002), which are also compared with velocity profiles gathered with the NSMP.

Table 5.1 Sites at which the BHS tests were performed

Province	Town	Station Code (GDDA)	Station Code (NSMP)	Dist. btw. MASW-BHS (m)	Depth of Exp. (m)
Kocaeli	Center	IZT	AI_004_IZT	5.0	20
Sakarya	Adapazarı	SKR	AI_005_SKR	3.0	30
Bolu	Göynük	GYN	AI_007_GYN_BHM	24.0	30
Bolu	Center	BOL	AI_010_BOL	27.3	28
Düzce	Center	DZC	AI_011_DZC	5.1	27
Bursa	İznik	IZN	AI_081_IZN_KY	41.8	30

Table 5.1 (Cont'd)

Province	Town	Station Code (GDDA)	Station Code (NSMP)	Dist. btw. MASW-BHS (m)	Depth of Exp. (m)
Canakkale	Center	CNK	AI_088_CNK	27.0	29
İzmir	Bornova	BRN	AI_115_BRN_BAY	81.9	30
Afyon	Dinar	DIN	AI_137_DIN	10.6	30

Table 5.2 Sites at which the SASW tests were performed

Province	Town	Station Code (GDDA)	Station Code (NSMP)	Depth of Exp. (m)
Kocaeli	Gebze	GBZ	AI_002_GBZ	25
Kocaeli	Center	IZT	AI_004_IZT	16
Sakarya	Adapazarı	SKR	AI_005_SKR	25
Bolu	Center	BOL	AI_010_BOL	40
Düzce	Center	DZC	AI_011_DZC	43
Bursa	İznik	IZN	AI_081_IZN_KY	15

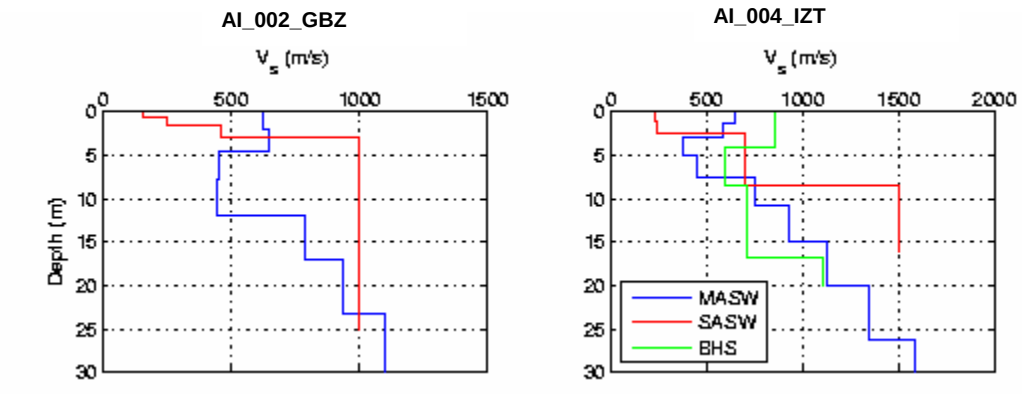

Figure 5.1 Comparison of V_s profiles obtained by MASW, SASW and BHS

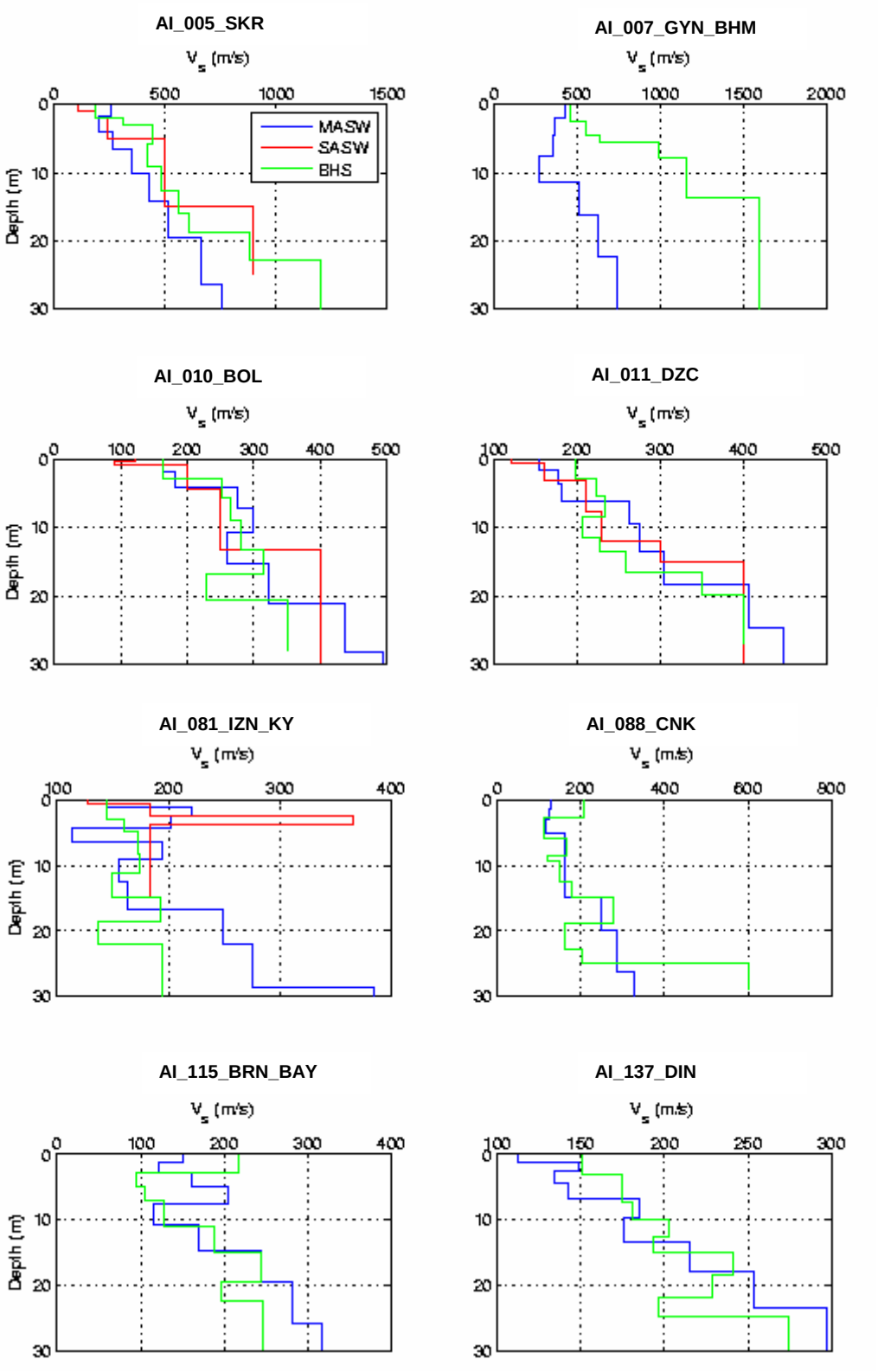

Figure 5.1 (Cont'd)

The V_s profiles obtained from MASW technique is compared with those obtained from BHS as well as those obtained from SASW. The comparisons are illustrated in Figure 5.1. It is noted that the obtained shear wave velocity profiles are very similar in case V_s < 400 m/s, however for stiff sites the differences between V_s profiles obtained from different tests can be substantial.

In addition to comparing V_s profiles, mean V_s of each site is compared as well. However, averaging over the uppermost 30 m of the profile is not applied, since the depths of exploration with BHS and SASW tests varied between 15 m and 30 m at each site. Considering these exploration depths of BHS test, Equation 3.1 is used for calculating mean V_s, however the $\sum d_i$ term in this equation is taken as the minimum exploration depth among the tests compared. Mean V_s obtained through MASW method ($V_{s,MASW}$), that obtained through BHS ($V_{s,BHS}$) and that obtained through SASW ($V_{s,SASW}$) are calculated. The $V_{s,30}$, $V_{s,MASW}$, $V_{s,BHS}$ and $V_{s,SASW}$ are presented in Table 5.3. Besides, relative percent difference (RPD) between $V_{s,MASW}$ and either $V_{s,SASW}$ or $V_{s,BHS}$ are given in Table 5.3.

The difference between $V_{s,MASW}$ and $V_{s,SASW}$ is less than 18% for all sites, whereas for two sites the difference between $V_{s,MASW}$ and $V_{s,BHS}$ is larger than 18%. Of these two sites, the first is AI_005_SKR with limestone formations with cavities inside, and the second is AI_007_GYN_BHM with excessive lateral heterogeneity (Yılmaz et al., 2008a).

The comparison of $V_{s,MASW}$ and $V_{s,BHS}$ is presented in Figure 5.2. The results from SASW and MASW are compared in Figure 5.3. The mean V_s of BHS sites for three methods are very similar except those calculated for the site AI_007_GYN_BHM. However, it is observed that as mean V_s increases, the discrepancy between results of MASW and BHS increases.

Table 5.3 Comparison of SASW, MASW and BHS results

Station Code (NSMP)	Min. Depth of Exp. (m)	$V_{s,30}$ (m/s)	$V_{s,MASW}$ (m/s)	$V_{s,SASW}$ (m/s)	$V_{s,BHS}$ (m/s)	RPD MASW- SASW	RPD MASW-BHS
AI_002_GBZ	25	701	653	760		16	-
AI_004_IZT	16	826	621	662	700	17	13
AI_005_SKR	25	412	379	430	472	13	25
AI_007_GYN_BHM	30	472	472		1055	-	124
AI_010_BOL	28	294	285	282	266	1	7
AI_011_DZC	27	282	271	266	266	2	2
AI_081_IZN_KY	15	197	161	189	159	17	1
AI_088_CNK	29	192	189		187	-	1
AI_115_BRN_BAY	30	196	196		175	-	11
AI_137_DIN	30	198	198		203	-	3

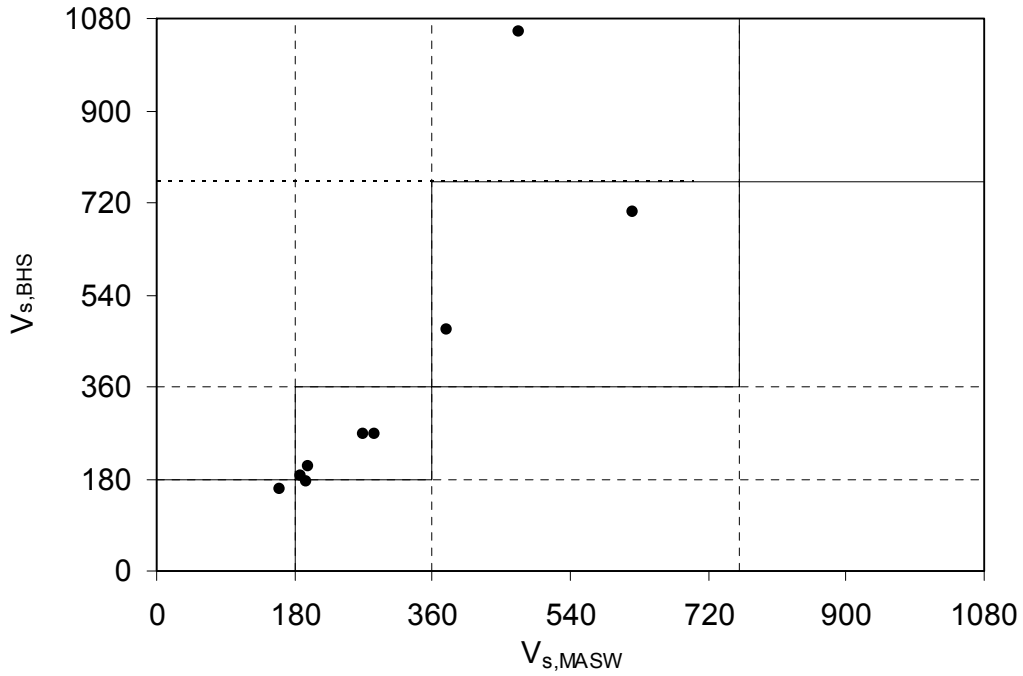

Figure 5.2 Comparison of mean V_s obtained by MASW and BHS

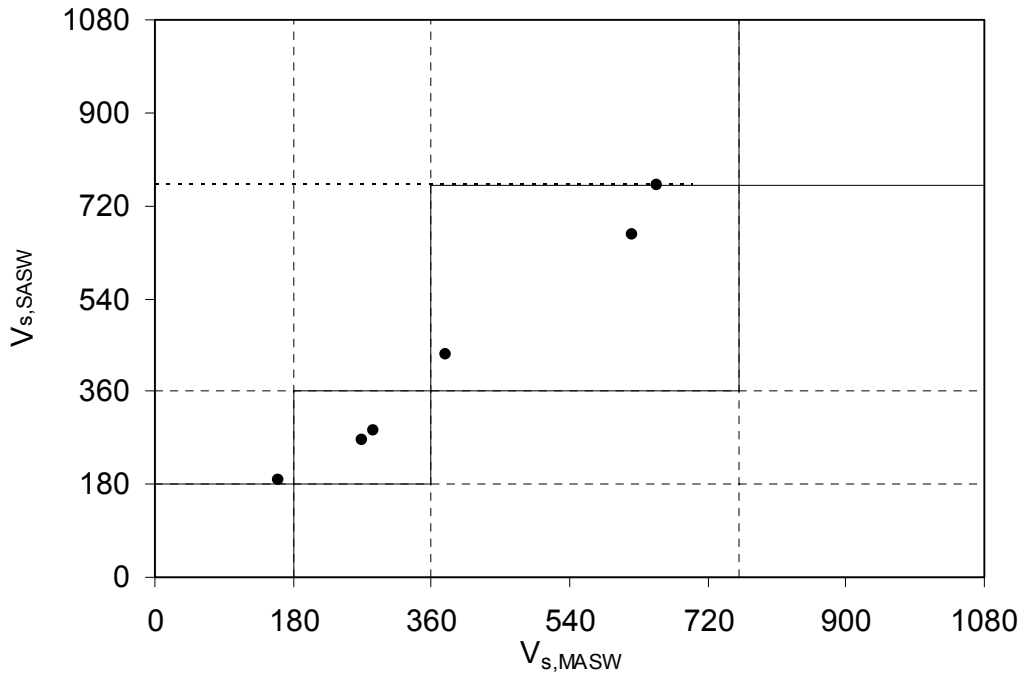

Figure 5.3 Comparison of mean V_s obtained by MASW and SASW

CHAPTER 6

SUMMARY AND CONCLUDING REMARKS

6.1 Summary

153 sites at which the strong-motion accelerographs are located were investigated through geophysical and geotechnical in-situ tests, within the scope of the project entitled “Compilation of National Strong Ground Motion Database in Accordance with International Standards”. The shear wave velocity profiles of the uppermost 30 m of sites were determined with MASW technique. In addition, variation of soil stiffness and description of soils were determined by SPT and lab tests on specimens. Core samples were also recovered from rock formations where encountered.

In this study, the seismic and geotechnical data is utilized to characterize the site conditions for the uppermost 30 m of the sites. NEHRP Provisions (BSSC, 2003), EC-8 (CEN, 2003) and TSDC (GDDA, 2007) are employed to classify the sites. The site classes are tabulated in Appendix A. The consistency between the site classes when seismic (V_s) and geotechnical (SPT) criteria are used is critically evaluated. The importance of SPT correction in site classification is investigated.

The liquefaction susceptibility of the sites with saturated sand is analyzed by employing the simplified procedure that assumes free field conditions. The analysis is applicable for soils shallower than 15 m. The liquefaction

susceptibility is expressed as peak horizontal ground acceleration necessary for triggering liquefaction for a magnitude (Mw) 7.5 event. The effect of variability in ground water level on liquefaction susceptibility is also investigated. Considering ground water level observed during borings, the liquefaction susceptibility of each site is given in Appendix B.

At selected nine sites borehole seismic test (BHS) was performed. Rosenblad et al. (2002) previously determined the Vs profiles at five of these sites by SASW method. The velocity profiles obtained after three different applications are compared.

6.2 Concluding Remarks

When NEHRP Provisions is employed for classification of NMSR sites the following conclusions are obtained:

- 56% of the sites are classified as class D, 42% are classified as class C and 2% are classified as class B utilizing the seismic (V_s) criterion. Besides, when geotechnical (SPT) criterion is employed, 45% of the sites are classified as class C, 50% are classified as class D and 5% are classified as class E.

- 74% of the sites are classified consistently according to both criteria. Furthermore, the 95% upper confidence limit (UCL) for the proportion of sites for which geotechnical criterion results in a softer site class than that determined by seismic criterion (i.e., unsafe classification by SPT criterion) is found as 9.8%.

- The 95% UCL for unsafe classifications are reduced to 6.5% when corrected SPT results are used. It is observed that correction for energy efficiency of hammer alone is sufficient.

- 64% of SPT refusals were observed when shear wave velocity of a layer is between 360 and 760 m/s. 58% of all SPT in gravels are refused. Reliability of SPT for classification of sites with gravelly soils apparently is less than those of sites with other types of soils.

- Instead of mean values for a site, when SPT and Vs of different soil levels are directly compared, it is observed that 87% of V_s and N data pairs are within consistent boundaries of NEHRP site classes.

The sites are also classified according to EC-8. The remarks for EC-8 are very similar to NEHRP Provisions. However, since there are some minor differences between the class boundaries defined on EC-8 and NEHRP for equivalent site classes, only the conclusions pertinent to site classification are given below:

- The distribution of site classes are 1%, 43%, 56% and 0% for class A, B, C and D, respectively according to seismic (V_s) criterion. The figures are 0%, 46%, 48% and 5% respectively when geotechnical (SPT) criterion is used.

TSDC has a very different classification system from NEHRP Provisions and EC-8. Since there are some difficulties in applying the TSDC criteria in very heterogeneous (i.e., stratified) soils, some additional rules are introduced in order to provide consistency in classification. The most important additional rule is that in extremely stratified soils the total thickness (instead of layer thickness) of the subclass is considered for site classification in case it is greater than 3 m. The conclusions can be summarized as in the following:

- Considering seismic criterion 153 sites are classified. The proportions of the sites corresponding to the classes Z1, Z2, Z3, and

Z4 are calculated as 1%, 36%, 56% and 5%, respectively. Whereas 94 sites are classified based on geotechnical criterion and the percentages of the classes are 26%, 52%, 21% and 1% respectively.

- SPT criterion resulted in stiffer site classes compared to that of Vs criterion.

- The consistency of N and V_s is evaluated for coarse- and fine-grained soils; the agreement is in order of 20-30%. It is apparent that SPT criterion in TSDC shall be modified.

- The Z3 sites determined by TSDC are generally grouped as site class D in NEHRP Provisions.

The liquefaction susceptibility analysis of NSMR-sites resulted in:

- 28 of NSMR-sites have liquefaction potential according to the simplified procedure for liquefaction potential analysis, when peak horizontal ground acceleration exceeds 0.4g for a magnitude 7.5 (M_w) event.

- If the GWL is shallower by 2 m, the number of sites with liquefaction potential will be increased to 37 for a magnitude 7.5 event.

Comparing the velocity profiles obtained by the application of SASW, MASW and BHS on selected sites, the following conclusions can be given:

- V_s profiles obtained by SASW are very similar to those obtained by MASW.

- The differences between velocity profiles pertinent to BHS and MASW results are tolerable except two of the sites. One of these is composed of a limestone formation and the other shows excessive lateral heterogeneity.

6.3 Future Studies

The recently compiled Turkish strong-motion database provides significant information for earthquake engineering and engineering seismology. In this study, the NSMR-sites are classified. With these results some future studies are discussed.

- Consistency between seismic and geotechnical criteria should be improved, especially for TSDC.

- The strong-motion records obtained from these sites shall be analyzed in order to determine the response spectrum shapes and site amplification factors, through developing new attenuation relationships with Turkish data.

- There exist a small number of NEHRP class A and B or class E sites in the database. Reliable estimation of either rock or soft soil spectrum lacks in this database. Hence, sites pertinent to these classes can be located by seismic and geotechnical tests, in order to deploy new accelerographs.

- The limitations of existing site classification systems in three codes should be investigated through employing strong motion records. Improvements on available criteria can be proposed.

REFERENCES

Aki, K., and Richards, P. G. (1980). *Quantitative seismology,* W.H. Freeman, CA.

Bakır, B. S., Yılmaz M. T., Yakut, A., and Gülkan, P. (2005). "Re-examination of damage distribution in Adapazarı: Geotechnical considerations" *Engineering Structures*, 27(7): 1002-1013.

Borcherdt, R. D. (1994). "Estimates of Site Dependent Response spectra for Design (Methodology and Justification)" *Earthquake Spectra*, 10(4): 617-653.

Bowles, J. E. (1996). *Foundation Analysis and Design,* McGraw Hill Inc., OH.

Budhu, M. (2000). *Soil mechanics and Foundations,* John Wiley and Sons Inc., MA.

Building Seismic Safety Council, BSSC (2003). "NEHRP Recommended Provisions for Seismic Regulations for New Buildings and Other Structures, Part 1 - Provisions and Part 2 - Commentary", Federal Emergency Management Agency, Washington D.C.

Bullen, K. E. (1965). *An introduction to the theory of seismology,* Cambridge Univ. Press, Cambridge.

Craig, R. F., (2002) *Soil Mechanics,* Spon Press, London.

Das, B. M. (2002). *Principles of Geotechnical Engineering*, Thomson Learning Inc., MA.

Devore, J. L. (2004). *Probability and Statistics for Engineers and the Sciences,* Thomson Learning Inc., MA.

Dobry, R., Borcherdt, R. D., Crouse, C. B., Idriss, I. M., Joyner, W. B., Martin, G. R., Power, M. S., Rinne, E. E., and Seed, R. B. (2000). "New site coefficients and site classification system used in recent building seismic code provisions," *Earthquake Spectra,* 16 (1): 41-67.

Erdoğan Ö. (2008). "Main Seismological Features of Recently Compiled Turkish Strong Motion Database" M. Sc. Thesis, Middle East Technical University, Ankara.

Erdoğdu, S. (2007). Personal communication.

European Committee for Standardization, CEN (2003). "Eurocode 8: Design of structures for earthquake resistance - Part 1: General rules, seismic actions and rules for buildings", European Committee for Standardization, Brussels.

General Directorate of Disaster Affairs (GDDA), (2007). "Turkish Seismic Design Code: Specification for Structures to be Built in Disaster Areas", General Directorate of Disaster Affairs, Ankara.

Kim, D-S. and Yoon, J-K. (2006). "Development of new site classification system for the regions of shallow bedrock in Korea" *Journal of Earthquake Engineering,* 10(3): 331–358.

Kramer, S. L. (1996). *Geotechnical Earthquake Engineering,* Prentice-Hall Inc, NJ.

Lee, C.-T., Cheng, C.-T., Liao, C.-W., and Tsai, Y.-B (2001). "Site classification of Taiwan free-field strong motion stations," *Bulletin of the Seismological Society of America,* 91(5): 1283-1297.

Orense, R. P. (2005). "Assessment of Liquefaction Potential Based on Peak Ground Motion Parameters" *Soil Dynamics and Earthquake Engineering*, 25: 225-240.

Park C. B., Miller R. D. and Xia J. (1997). "Multi-channel analysis of surface waves (MASW) ~ A summary report of technical aspects, experimental results, and perspective ~" Kansas Geological Survey *Open-file Report No #97-10*, KS.

Park C. B., Miller R. D. and Xia J. (1999). "Multi-channel analysis of surface waves" *Geophysics*, 64(3): 800-808.

Phung V., Atkinson, G. M., and Lau, D. T. (2006). "Methodology for Site Classification Estimation Using Strong Ground Motion Data from the Chi-Chi, Taiwan, Earthquake" *Earthquake Spectra,* 22(2): 511-531.

Rathje, E. M., Stokoe II, K. H., and Rosenblad, B. (2003). "Strong motion station characterization and site effects during the 1999 earthquakes in Turkey," *Earthquake Spectr*a, 19(3): 653-675.

Rodriguez-Marek, A., Bray, J. D., and Abrahamson N. A. (2001). "An empirical geotechnical seismic site response procedure" *Earthquake Spectra,* 17(1): 65-87.

Rosenblad, B. L., Rathje, E. M., and Stokoe, K. H. (2002). “Shear wave velocity profiling by SASW method at selected strong-Motion stations in Turkey” *Lifelines Projects Topic 2 – Site Response Report No. 2A02a,* Pacific Earthquake Engineering Research Center, California.

Seed, H. B. (1979). “Soil Liquefaction and Cyclic Mobility Evaluation for Level Ground During Earthquakes” *Journal of Geotechnical Engineering Division*, 105(2): 201–255.

Seed, H. B., and Idriss, I. M. (1971) “Simplified Procedure for Evaluating Soil Liquefaction Potential” *Journal of Soil Mechanics and Foundation Division,* 97(9): 1249-1273.

Seed, H. B., and Idriss, I. M. (1982) “Ground Motions and Soil Liquefaction during Earthquakes” Earthquake Engineering Research Institute Monograph.

Seed, H. B., Tokimatsu, K., Harder, L. F., and Chung, R. M. (1985) “The Influence of SPT Procedures in Soil Liquefaction Resistance Evaluations” *Journal of Geotechnical Engineering*, 111(12): 1425-1445.

Seed, H. B., Ugas, C. and Lysmer, J. (1976). “Site-dependent spectra for earthquake-resistant design” *Bulletin of the Seismological Society of America,* 66(1): 221-244.

Sivrikaya, O., and Toğrol, E. (2006). “Determination of undrained strength of fine-grained soils by means of SPT and its application in Turkey” *Engineering Geology*, 86(1): 52-69.

Stewart, J. P., Liu, A. H., Choi, Y., and Baturay, M. B. (2001). “Amplification factors for spectral acceleration in active regions,” *Report No. PEER-2001/10,* Pacific Earthquake Engineering Research Center, California.

Xia J., Miller R. D., and Park C. B. (1999). “Estimation of near-surface shear-wave velocity by inversion of Rayleigh waves” *Geophysics*, 64(3): 691-700.

Xia J., Miller R. D., Park C. B., and Tian G. (2002). “Comparing shear wave velocity profiles inverted from multichannel surface wave with borehole measurements” *Soil Dynamics and Earthquake Engineering*, 22: 181-190.

Xia J., Miller R. D., Park C. B., and Tian G. (2003). “Inversion of high frequency surface waves with fundamental and higher modes” *Journal of Applied Geophysics*, 52: 45-57.

Xia J., Miller R. D., Park C. B., Tian G., and Chen C. (2004). “Utilization of high frequency Rayleigh waves in near-surface geophysics” *The Leading Edge*, 23: 753-759.

Xia J., Xu., Y., Miller R. D., and Chen C. (2006). “Estimation of elastic moduli in a compressible Gibson half-space by inverting Rayleigh wave phase velocity” *Surveys in Geophysics*, 27: 1-17.

Yılmaz, M. T. (1999). “Mapping Liquefaction Susceptibility of the İzmir Metropolitan Area” M. Sc. Thesis, Middle East Technical University, Ankara.

Yılmaz, Ö., Eser, M. and Berilgen, M. (2007). “Applications of engineering seismology for site characterization” *4th International Conference on Geotechnical Earthquake Engineering,* Thessaloniki.

Yılmaz, Ö., Eser, M., Sandıkkaya, M. A., Akkar, S., Yılmaz, M. T., and Bakır, B. S. (2008a). “Comparison of Shear-Wave Velocity-Depth Profiles from Downhole and Surface Seismic Experiments” *14th World Conference on Earthquake Engineering*, Beijing (In press).

Yılmaz, Ö., Savaşkan, E., Bakır, B. S., Yılmaz, M. T., Eser, M. , Akkar, S., Tüzel, B., İravul, Y., Özmen, Ö. T., Denizlioğlu, A. Z., Alkan, A., and Gürbüz, M. (2008b). “Shallow Seismic and Geotechnical Site Surveys at the Turkish National Grid for Strong-Motion Seismograph Stations” 14th *World Conference on Earthquake Engineering*, Beijing (In press).

Youd T. L., et al. (2001). “Liquefaction Resistance of Soils: Summary Report from the 1996 NCEER and 1998 NCEER/NSF Workshops on Evaluation of Liquefaction Resistance of Soils” *Journal of Geotechnical and Geoenvironmental Engineering,* 127(10): 817-833.

Zare, M. and Bard, P-Y. (2002). “Strong motion dataset of Turkey: data processing” and site classification” *Soil Dynamics and Earthquake Engineering,* 22(8): 703–718.

APPENDIX A

SITE INFORMATION FOR STATIONS

Table A.1 List of the stations

No	Station Code NSMP	Station Code GDDA (old)	Station Code GDDA (new)	Station Province
1	AI_001_IST	IST	3401	İstanbul / Merkez
2	AI_002_GBZ	GBZ	4106	Kocaeli / Gebze
3	AI_003_IZN	IZN	1611	Bursa / İznik
4	AI_004_IZT	IZT	4101	Kocaeli / Merkez
5	AI_005_SKR	SKR	5401	Sakarya / Merkez
6	AI_006_AKY	AKY	5402	Sakarya / Akyazı
7	AI_007_GYN_BHM	GYN	1403	Bolu / Göynük
8	AI_008_GYN_DH	GYN	1404	Bolu / Göynük
9	AI_009_MDR	MDR	1406	Bolu / Mudurnu
10	AI_010_BOL	BOL	1401	Bolu / Merkez
11	AI_011_DZC	DZC	8101	Düzce / Merkez
12	AI_012_MEN	MEN	1405	Bolu / Mengen
13	AI_013_CER	CER	1801	Çankırı / Çerkeş
14	AI_014_KBK	KBK	7801	Karabük / Merkez
15	AI_015_GRD	GRD	1402	Bolu / Gerede
16	AI_016_BEY	BEY	0601	Ankara / Beypazarı
17	AI_017_HAY	HAY	0602	Ankara / Haymana
18	AI_018_CMR	CMR	5101	Niğde / Çamardı
19	AI_019_MRS	MRS	3301	Mersin / Merkez
20	AI_020_KRT	KRT	0110	Adana / Karataş
21	AI_021_CYH_PTT	CYH	0104	Adana / Ceyhan
22	AI_022_CYH_TIM	CYH	0105	Adana / Ceyhan
23	AI_023_MAT17	MAT17	8001	Osmaniye / Merkez
24	AI_024_MAT18	MAT18	8002	Osmaniye / Bahçe
25	AI_025_MAT06_MET	MAT06	3106	Hatay / İskenderun
26	AI_026_MAT06_MIM	MAT06	3107	Hatay / İskenderun
27	AI_027_MAT01	MAT01	3110	Hatay / Samandağ
28	AI_028_MAT03	MAT03	3101	Hatay / Merkez
29	AI_029_MAT02	MAT02	3103	Hatay / Altınözü

Table A.1 (Cont'd)

No	Station Code NSMP	Station Code GDDA (old)	Station Code GDDA (new)	Station Province
29	AI_029_MAT02	MAT02	3103	Hatay / Altınözü
30	AI_030_MAT04	MAT04	3111	Hatay / Serinyol
31	AI_031_MAT05	MAT05	3108	Hatay / Kırıkhan
32	AI_032_MAT07	MAT07	3109	Hatay / Kırıkhan
33	AI_033_MAT08	MAT08	3104	Hatay / Hassa
34	AI_034_MAT09	MAT09	3105	Hatay / Hassa
35	AI_035_MAT15	MAT15	2701	G.Antep / İslahiye
36	AI_036_MAT16	MAT16	2702	G.Antep / Nurdağı
37	AI_037_MAT13	MAT13	4608	K.Maraş / Türkoğlu
38	AI_038_MAT14	MAT14	4606	K.Maraş / Narlı
39	AI_039_AND	AND	4604	K.Maraş / Andırın
40	AI_040_ELB	ELB	4605	K.Maraş / Elbistan
41	AI_041_MAT11	MAT11	4601	K.Maraş / Merkez
42	AI_042_MAT12_MET	MAT12	4602	K.Maraş / Merkez
43	AI_043_KMR	KMR	4603	K.Maraş / Merkez
44	AI_044_MAT10	MAT10	4607	K.Maraş / Pazarcık
45	AI_045_GOL	GOL	0202	Adıyaman / Gölbaşı
46	AI_046_DSH	DSH	4403	Malatya / Doğanşehir
47	AI_047_MLT	MLT	4401	Malatya / Merkez
48	AI_048_ELZ	ELZ	2301	Elazığ / Merkez
49	AI_049_BNG	BNG	1201	Bingöl / Merkez
50	AI_050_SLH_OE	SLH	1208	Bingöl / Solhan
51	AI_051_SLH_MET	SLH	1209	Bingöl / Solhan
52	AI_052_MUS	MUS	4901	Muş / Merkez
53	AI_053_MLZ	MLZ	4902	Muş / Malazgirt
54	AI_054_TAT	TAT	1301	Bitlis / Tatvan
55	AI_055_VAN	VAN	6501	Van / Merkez
56	AI_056_MUR	MUR	6502	Van / Muradiye
57	AI_057_DBY	DBY	0402	Ağrı / Doğubeyazıt
58	AI_058_AGR	AGR	0401	Ağrı / Merkez
59	AI_059_HRS	HRS	2503	Erzurum / Horasan
60	AI_060_KRS	KRS	3601	Kars / Merkez
61	AI_061_ARD	ARD	7501	Ardahan / Merkez
62	AI_062_ERZ	ERZ	2501	Erzurum / Merkez
63	AI_063_TER_MET	TER	2405	Erzincan / Tercan
64	AI_064_TER_PTT	TER	2406	Erzincan / Tercan
65	AI_065_ERC	ERC	2401	Erzincan / Merkez
66	AI_066_ZAR	ZAR	5802	Sivas / Zara
67	AI_067_REF_HK	REF	2403	Erzincan / Refahiye
68	AI_068_REF_KM	REF	2404	Erzincan / Refahiye
69	AI_069_SSH	SSH	5801	Sivas / Suşehri
70	AI_070_RES	RES	6004	Tokat / Reşadiye
71	AI_071_TKT	TKT	6001	Tokat / Merkez

Table A.1 (Cont'd)

No	Station Code NSMP	Station Code GDDA (old)	Station Code GDDA (new)	Station Province
72	AI_072_ERB	ERB	6003	Tokat / Erbaa
73	AI_073_AMS_MZFL	AMS	0501	Amasya / Merkez
74	AI_074_AMS_BAY	AMS	0502	Amasya / Merkez
75	AI_075_MRZ	MRZ	0504	Amasya / Merzifon
76	AI_076_OSM_BEL	OSM	1902	Çorum / Osmancık
77	AI_077_OSM_EHK	OSM	1903	Çorum / Osmancık
78	AI_078_KRG	KRG	1901	Çorum / Kargı
79	AI_079_TOS	TOS	3701	Kastamonu / Tosya
80	AI_080_YLV	YLV	7705	Yalova / Merkez
81	AI_081_IZN_KY	IZN	1612	Bursa / İznik
82	AI_082_CEK	CEK	3403	İstanbul / K.Çekmece
83	AI_083_ERG	ERG	5903	Tekirdağ / Marmara Ereğlisi
84	AI_084_TKR_MET	TKR	5901	Tekirdağ / Merkez
85	AI_085_TKR_HK	TKR	5902	Tekirdağ / Merkez
86	AI_086_SRK	SRK	5904	Tekirdağ / Şarköy
87	AI_087_GL1	GL-1	1705	Çanakkale / Gelibolu
88	AI_088_CNK	CNK	1701	Çanakkale / Merkez
89	AI_089_KRB	KRB	1706	Çanakkale / Karabiga
90	AI_090_BGA	BGA	1703	Çanakkale / Biga
91	AI_091_GNN	GNN	1014	Balıkesir / Gönen
92	AI_092_EDN_SO	EDN	1011	Balıkesir / Edincik
93	AI_093_EDN_KGI	EDN	1012	Balıkesir / Edincik
94	AI_094_YNC	YNC	1707	Çanakkale / Yenice
95	AI_095_EZN	EZN	1704	Çanakkale / Ezine
96	AI_096_EDR	EDR	1013	Balıkesir / Edremit
97	AI_097_AYV	AYV	1005	Balıkesir / Ayvalık
98	AI_098_DKL	DKL	3503	İzmir / Dikili
99	AI_099_KNK	KNK	3508	İzmir / Kınık
100	AI_100_AKS	AKS	4502	Manisa / Akhisar
101	AI_101_GOR	GOR	4505	Manisa / Gördes
102	AI_102_DMR	DMR	4504	Manisa / Demirci
103	AI_103_SMV	SMV	4305	Kütahya / Simav
104	AI_104_GDZ	GDZ	4304	Kütahya / Gediz
105	AI_105_USK	USK	6401	Uşak / Merkez
106	AI_106_BLD	BLD	2003	Denizli / Buldan
107	AI_107_DNZ_MET	DNZ	2001	Denizli / Merkez
108	AI_108_DNZ_BAY	DNZ	2002	Denizli / Merkez
109	AI_109_ALA	ALA	4503	Manisa / Alaşehir
110	AI_110_SAL	SAL	4506	Manisa / Salihli
111	AI_111_ODM	ODM	3509	İzmir / Ödemiş
112	AI_112_MNS	MNS	4501	Manisa / Merkez
113	AI_113_FOC	FOC	3504	İzmir / Foça
114	AI_114_GZL_MET	GZL	3506	İzmir / Güzelyalı

Table A.1 (Cont'd)

No	Station Code NSMP	Station Code GDDA (old)	Station Code GDDA (new)	Station Province
115	AI_115_BRN_BAY	BRN	3501	İzmir / Bornova
116	AI_116_BRN_EU	BRN	3502	İzmir / Bornova
117	AI_117_KUS_MET	KUS	0905	Aydın / Kuşadası
118	AI_118_KUS_HSL	KUS	0906	Aydın / Kuşadası
119	AI_119_AYD_HH	AYD	0901	Aydın / Merkez
120	AI_120_AYD_DSI	AYD	0902	Aydın / Merkez
121	AI_121_BDR	BDR	4802	Muğla / Bodrum
122	AI_122_MLS	MLS	4806	Muğla / Milas
123	AI_123_YTG	YTG	4807	Muğla / Yatağan
124	AI_124_YER	YER	4808	Muğla / Yerkesik
125	AI_125_MAR	MAR	4805	Muğla / Marmaris
126	AI_126_KOY	KOY	4804	Muğla / Köyçeğiz
127	AI_127_FTH	FTH	4803	Muğla / Fethiye
128	AI_128_CAM	CAM	2004	Denizli / Çameli
129	AI_129_FNK	FNK	0703	Antalya / Finike
130	AI_130_BCK_KGI	BCK	1503	Burdur / Bucak
131	AI_131_BCK_OM	BCK	1504	Burdur / Bucak
132	AI_132_TFN	TFN	1505	Burdur / Tefenni
133	AI_133_BRD1	BRD-1	1501	Burdur / Merkez
134	AI_134_BRD2	BRD-2	1502	Burdur / Merkez
135	AI_135_SNK	SNK	3201	Isparta / Senirkent
136	AI_136_CRD	CRD	2005	Denizli / Çardak
137	AI_137_DIN	DIN	0302	Afyon / Dinar
138	AI_138_SDL	SDL	0308	Afyon / Sandıklı
139	AI_139_AFY	AFY	0301	Afyon / Merkez
140	AI_140_STG	STG	2609	Eskişehir / Seyitgazi
141	AI_141_KUT_BAY	KUT	4301	Kütahya / Merkez
142	AI_142_KUT_SS	KUT	4302	Kütahya / Merkez
143	AI_143_EMT	EMT	4303	Kütahya / Emet
144	AI_144_DUR_MET	DRSB	1009	Balıkesir / Dursunbey
145	AI_145_DUR_KGI	DUR	1010	Balıkesir / Dursunbey
146	AI_146_BLK	BLK	1001	Balıkesir / Merkez
147	AI_147_BGC	BGC	1008	Balıkesir / Bigadiç
148	AI_148_SNG	SNG	1015	Balıkesir / Sındırgı
149	AI_149_BND_MET	BND	1006	Balıkesir / Bandırma
150	AI_150_BND_TDM	BND	1007	Balıkesir / Bandırma
151	AI_151_MKP	MKP	1614	Bursa / M.Kemal Paşa
152	AI_152_BYT02	BYT02	1601	Bursa / Merkez
153	AI_153_ING	ING	1610	Bursa / İnegöl

Table A.2 Location of the stations

Station Code NSMP	Location of the Station
AI_001_IST	Bayındırlık ve İskan Müdürlüğü
AI_002_GBZ	Tübitak Marmara Araştırma Merkezi
AI_003_IZN	Hükümet Konağı
AI_004_IZT	Meteoroloji İstasyon Müdürlüğü
AI_005_SKR	Bayındırlık ve İskan Müdürlüğü
AI_006_AKY	Orman İşletme Müdürlüğü
AI_007_GYN_BHM	Belediye Hava Meydanları
AI_008_GYN_DH	Göynük Devlet Hastanesi
AI_009_MDR	PTT Binası
AI_010_BOL	Bayındırlık ve İskan Müdürlüğü
AI_011_DZC	Meteoroloji İstasyon Müdürlüğü
AI_012_MEN	PTT Binası
AI_013_CER	Meteoroloji İstasyon Müdürlüğü
AI_014_KBK	Karabük Anadolu Lisesi
AI_015_GRD	Orman İşletme Müdürlüğü
AI_016_BEY	Meteoroloji İstasyon Müdürlüğü
AI_017_HAY	Doğan İlköğretim Okulu
AI_018_CMR	Emniyet Müdürlüğü Arşivi
AI_019_MRS	Meteoroloji İstasyon Müdürlüğü
AI_020_KRT	Meteoroloji İstasyon Müdürlüğü
AI_021_CYH_PTT	PTT Müdürlüğü
AI_022_CYH_TIM	Tarım İlçe Müdürlüğü
AI_023_MAT17	DSİ İşletme Baş Mühendisliği
AI_024_MAT18	Çok Programlı Lise Bahçesi
AI_025_MAT06_MET	Meteoroloji Müdürlüğü
AI_026_MAT06_MIM	Meyvecilik Üretme İstasyon Müdürlüğü Bahçesi
AI_027_MAT01	Meteoroloji İstasyon Müdürlüğü
AI_028_MAT03	Köy Hizmetleri Müdürlüğü Bahçesi
AI_029_MAT02	Tarım Müdürlüğü Bahçesi
AI_030_MAT04	Orman Fidanlık Müdürlüğü Bahçesi
AI_031_MAT05	75.Yıl Anaokulu Bahçesi
AI_032_MAT07	Güzelce Köyü Sağlıkevi Bahçesi
AI_033_MAT08	Aktepe Sağlık Ocağı Bahçesi
AI_034_MAT09	Merkez Sağlık Ocağı Bahçesi
AI_035_MAT15	Meteoroloji İstasyon Müdürlüğü
AI_036_MAT16	Merkez Sağlık Ocağı Bahçesi
AI_037_MAT13	Dr. Kemal Beyazıt Fizik Tedavi Ve Rehabilitasyon Merkezi Bahçesi
AI_038_MAT14	Çukobirlik Kooperatifi Bahçesi
AI_039_AND	Tufan Paşa İlköğretim Okulu
AI_040_ELB	Meteoroloji İstasyon Müdürlüğü
AI_041_MAT11	DSİ 20. Bölge Müdürlüğü Bahçesi
AI_042_MAT12_MET	Meteoroloji İstasyon Müdürlüğü
AI_043_KMR	Bayındırlık ve İskan Müdürlüğü

Table A.2 (Cont'd)

Station Code NSMP	Location of the Station
AI_044_MAT10	1 Nolu Sağlık Ocağı
AI_045_GOL	Meteoroloji İstasyon Müdürlüğü
AI_046_DSH	Meteoroloji İstasyon Müdürlüğü
AI_047_MLT	Bayındırlık ve İskan Müdürlüğü
AI_048_ELZ	Bayındırlık ve İskan Müdürlüğü
AI_049_BNG	Bayındırlık ve İskan Müdürlüğü
AI_050_SLH_OE	Öğretmen Evi
AI_051_SLH_MET	Meteoroloji Müdürlüğü
AI_052_MUS	Bayındırlık ve İskan Müdürlüğü
AI_053_MLZ	Meteoroloji İstasyon Müdürlüğü
AI_054_TAT	Meteoroloji İstasyon Müdürlüğü
AI_055_VAN	Bayındırlık ve İskan Müdürlüğü
AI_056_MUR	Meteoroloji Müdürlüğü
AI_057_DBY	Meteoroloji İstasyon Müdürlüğü
AI_058_AGR	Bayındırlık ve İskan Müdürlüğü
AI_059_HRS	Meteoroloji İstasyon Müdürlüğü
AI_060_KRS	Bayındırlık ve İskan Müdürlüğü
AI_061_ARD	Meteoroloji Müdürlüğü
AI_062_ERZ	Bayındırlık ve İskan Müdürlüğü
AI_063_TER_MET	Meteoroloji Müdürlüğü
AI_064_TER_PTT	PTT Binası
AI_065_ERC	Bayındırlık ve İskan Müdürlüğü
AI_066_ZAR	Meteoroloji İstasyon Müdürlüğü
AI_067_REF_HK	Hükümet Konağı
AI_068_REF_KM	Kültür Merkezi
AI_069_SSH	DSİ 192. Şube Müdürlüğü
AI_070_RES	Termal Otel
AI_071_TKT	Devlet Su İşleri 72. Şube Müdürlüğü
AI_072_ERB	Belediye Seracılık Binası
AI_073_AMS_MZFL	Macit Zeren Fen Lisesi
AI_074_AMS_BAY	Bayındırlık ve İskan Müdürlüğü
AI_075_MRZ	Meteoroloji İstasyon Müdürlüğü
AI_076_OSM_BEL	Belediye Binası
AI_077_OSM_EHK	Eski Hükümet Konağı
AI_078_KRG	Orman İşletme Müdürlüğü
AI_079_TOS	Meteoroloji İstasyon Müdürlüğü
AI_080_YLV	Meteoroloji Müdürlüğü
AI_081_IZN_KY	Karayolları 147. Şube Şefliği
AI_082_CEK	Nükleer Santral Binası
AI_083_ERG	Kaymakamlık Binası
AI_084_TKR_MET	Meteoroloji Müdürlüğü
AI_085_TKR_HK	Valilik Binası
AI_086_SRK	Sağlık Ocağı Bahçesi

Table A.2 (Cont'd)

Station Code NSMP	Location of the Station
AI_087_GL1	Karayolları 13. Şube Şefliği
AI_088_CNK	Meteoroloji İstasyon Müdürlüğü
AI_089_KRB	Belediye Binası
AI_090_BGA	İlçe Tarım Müdürlüğü
AI_091_GNN	Meteoroloji İstasyon Müdürlüğü
AI_092_EDN_SO	Sağlık Ocağı
AI_093_EDN_KGI	Kandilli Gözlem İstasyonu
AI_094_YNC	Hükümet Konağı
AI_095_EZN	Meteoroloji İstasyon Müdürlüğü
AI_096_EDR	Meteoroloji İstasyon Müdürlüğü
AI_097_AYV	Meteoroloji İstasyon Müdürlüğü
AI_098_DKL	Meteoroloji İstasyon Müdürlüğü
AI_099_KNK	İtfaiye Amirliği
AI_100_AKS	Meteoroloji İstasyon Müdürlüğü
AI_101_GOR	Orman İşletme Müdürlüğü
AI_102_DMR	Meteoroloji İstasyon Müdürlüğü
AI_103_SMV	Meteoroloji İstasyon Müdürlüğü
AI_104_GDZ	Meteoroloji İstasyon Müdürlüğü
AI_105_USK	Meteoroloji İstasyon Müdürlüğü
AI_106_BLD	Kaymakamlık Binası
AI_107_DNZ_MET	Meteoroloji Müdürlüğü
AI_108_DNZ_BAY	Bayındırlık ve İskan Müdürlüğü
AI_109_ALA	İlçe Tarım Müdürlüğü
AI_110_SAL	Meteoroloji İstasyon Müdürlüğü
AI_111_ODM	Meteoroloji İstasyon Müdürlüğü
AI_112_MNS	Bayındırlık ve İskan Müdürlüğü
AI_113_FOC	Sağlık Ocağı
AI_114_GZL_MET	Meteoroloji Müdürlüğü
AI_115_BRN_BAY	Bayındırlık ve İskan Müdürlüğü
AI_116_BRN_EU	Ege Üniversitesi Ziraat Fakültesi
AI_117_KUS_MET	Meteoroloji Müdürlüğü
AI_118_KUS_HSL	Halk Sağlığı Laboratuvarı
AI_119_AYD_HH	Tarım ve Köy İşleri Bakanlığı Hayvan Sağlığı Şube Müdürlüğü
AI_120_AYD_DSI	Devlet Su İşleri 6. Bölge Müdürlüğü
AI_121_BDR	Meteoroloji İstasyon Müdürlüğü
AI_122_MLS	Meteoroloji İstasyon Müdürlüğü
AI_123_YTG	Meteoroloji İstasyon Müdürlüğü
AI_124_YER	Kandilli Gözlem İstasyonu
AI_125_MAR	Meteoroloji İstasyon Müdürlüğü
AI_126_KOY	Meteoroloji İstasyon Müdürlüğü
AI_127_FTH	Meteoroloji İstasyon Müdürlüğü
AI_128_CAM	Orman İşletme Müdürlüğü
AI_129_FNK	Meteoroloji İstasyon Müdürlüğü

Table A.2 (Cont'd)

Station Code NSMP	Location of the Station
AI_130_BCK_KGI	Kandilli Gözlem İstasyonu
AI_131_BCK_OM	Orman İşletme Müdürlüğü
AI_132_TFN	Meteoroloji İstasyon Müdürlüğü
AI_133_BRD1	Meteoroloji İstasyon Müdürlüğü
AI_134_BRD2	Bayındırlık ve İskan Müdürlüğü
AI_135_SNK	Meteoroloji İstasyon Müdürlüğü
AI_136_CRD	Meteoroloji İstasyon Müdürlüğü
AI_137_DIN	Meteoroloji İstasyon Müdürlüğü
AI_138_SDL	Karayolları Şube Şefliği
AI_139_AFY	Bayındırlık ve İskan Müdürlüğü
AI_140_STG	Kaymakamlık Binası
AI_141_KUT_BAY	Bayındırlık ve İskan Müdürlüğü
AI_142_KUT_SS	Sivil Savunma Müdürlüğü
AI_143_EMT	Karayolları 148.Şube Müdürlüğü
AI_144_DUR_MET	Meteoroloji Müdürlüğü
AI_145_DUR_KGI	Kandilli Gözlem İstasyonu
AI_146_BLK	Balıkesir Huzurevi
AI_147_BGC	Devlet Su İşleri İşletme Müdürlüğü
AI_148_SNG	Belediye Ziraat Bahçesi
AI_149_BND_MET	Meteoroloji Müdürlüğü
AI_150_BND_TDM	Bölge Trafik Denetleme Müdürlüğü
AI_151_MKP	Orman İşletme Müdürlüğü
AI_152_BYT02	Afet Yönetim Merkezi
AI_153_ING	Tarım İlçe Müdürlüğü

Table A.3 Geographical Coordinates of the Stations

Station Code	Seis. Latitude	Seis. Longitude	CSL Latitude	CSL Longitude	Borehole Latitude	Borehole Longitude	Distance btw. Seis. and CSL (m)	Distance btw. Seis. and Borehole (m)	Distance btw. Borehole and CSL (m)	Altitude (m)
AI_001_IST	41.05820	29.00951	41.05786	29.00866	41.05815	29.00932	92	20	72	130
AI_002_GBZ	40.78627	29.45003	40.78665	29.45095	40.78653	29.45052	100	55	45	198
AI_003_IZN	40.42993	29.71945	40.42951	29.71853	40.42963	29.71950	101	30	98	99
AI_004_IZT	40.76650	29.91721	40.76653	29.91811	40.76673	29.91712	90	25	101	77
AI_005_SKR	40.73707	30.38005	40.73663	30.38078	40.73660	30.38078	85	87	3	46
AI_006_AKY	40.67030	30.62250	40.67046	30.62330	40.67046	30.62333	82	85	3	52
AI_007_GYN_BHM	40.39842	30.78975	40.39855	30.79015	40.39856	30.78991	42	21	24	825
AI_008_GYN_DH	40.39659	30.78307	40.39688	30.78321	40.39660	30.78320	32	13	28	744
AI_009_MDR	40.46843	31.20994	40.46831	31.21013	40.46858	31.20994	22	15	33	831
AI_010_BOL	40.74567	31.60732	40.74635	31.60755	40.74636	31.60757	72	73	2	746
AI_011_DZC	40.84364	31.14888	40.84366	31.14838	40.84363	31.14844	50	44	7	145
AI_012_MEN	40.93811	32.07602	40.93836	32.07690	40.93820	32.07679	91	78	19	623
AI_013_CER	40.81486	32.88337	40.81570	32.88326	40.81567	32.88327	85	82	3	1137
AI_014_KBK	41.20455	32.62372	41.20536	32.62318	41.20543	32.62317	97	104	7	302
AI_015_GRD	40.79248	32.20593	40.79293	32.20526	40.79308	32.20540	81	80	21	1305
AI_016_BEY	40.16078	31.91698	40.16083	31.91741	40.16103	31.91687	43	27	58	684
AI_017_HAY	39.43994	32.50636	39.43986	32.50691	39.43993	32.50684	56	48	10	1254
AI_018_CMR	37.83196	34.98685	37.83213	34.98706	37.83178	34.98705	27	27	35	1496
AI_019_MRS	36.78098	34.60277	36.78160	34.60151	36.78095	34.60281	140	5	145	4
AI_020_KRT	36.56801	35.39008	36.56766	35.38973	36.56795	35.39028	49	21	62	22
AI_021_CYH_PTT	37.02403	35.80947	37.02436	35.80821	37.02407	35.80942	130	6	124	38
AI_022_CYH_TIM	37.02670	35.81624	37.02651	35.81631	37.02667	35.81597	20	27	38	36
AI_023_MAT17	37.08417	36.26936	37.08383	36.26913	37.08420	36.26932	41	5	42	122
AI_024_MAT18	37.19156	36.56195	37.19106	36.56210	37.19149	36.56202	52	10	44	593
AI_025_MAT06_MET	36.59229	36.15826	36.59301	36.15886	36.59239	36.15844	94	21	75	2

Table A3 (Cont'd)

Station Code	Seis. Latitude	Seis. Longitude	CSL Latitude	CSL Longitude	Borehole Latitude	Borehole Longitude	Distance btw. Seis. and CSL (m)	Distance btw. Seis. and Borehole (m)	Distance btw. Borehole and CSL (m)	Altitude (m)
AI_026_MAT06_MIM	36.58211	36.18491	36.58206	36.18426	36.58214	36.18478	65	13	53	10
AI_027_MAT01	36.08155	35.94982	36.08145	35.94901	36.08167	35.94980	82	12	82	3
AI_028_MAT03	36.21423	36.15973	36.21461	36.15991	36.21474	36.15954	42	54	39	85
AI_029_MAT02	36.11593	36.24722	36.11583	36.24736	36.11592	36.24719	17	3	19	269
AI_030_MAT04	36.37260	36.21973	36.37276	36.21926	36.37267	36.21963	50	12	38	111
AI_031_MAT05	36.49797	36.36612	36.49826	36.36621	36.49810	36.36613	30	13	18	139
AI_032_MAT07	36.58383	36.41439	36.58408	36.41495	36.58407	36.41461	61	33	34	109
AI_033_MAT08	36.69293	36.48852	36.69273	36.48908	36.69271	36.48893	59	47	15	260
AI_034_MAT09	36.80262	36.51119	36.80253	36.51080	36.80257	36.51110	40	10	30	459
AI_035_MAT15	37.02546	36.63593	37.02541	36.63545	37.02566	36.63441	48	153	107	522
AI_036_MAT16	37.18430	36.73280	37.18478	36.73250	37.18434	36.73287	57	8	57	538
AI_037_MAT13	37.37547	36.83836	37.37548	36.83841	37.37551	36.83855	5	19	14	499
AI_038_MAT14	37.38676	37.13803	37.38765	37.13865	37.38761	37.13802	108	85	63	581
AI_039_AND	37.57010	36.35737	37.57018	36.35716	37.57007	36.35727	22	10	16	965
AI_040_ELB	38.20368	37.19771	38.20358	37.19810	38.20356	37.19788	40	21	22	1133
AI_041_MAT11	37.53872	36.98187	37.53955	36.98213	37.53926	36.98168	87	57	54	549
AI_042_MAT12_MET	37.57532	36.91505	37.57565	36.91483	37.57547	36.91493	40	19	21	572
AI_043_KMR	37.57998	36.93061	37.57963	36.93041	37.57976	36.93056	40	23	20	562
AI_044_MAT10	37.48513	37.29775	37.48486	37.29785	37.48489	37.29783	29	25	4	771
AI_045_GOL	37.78694	37.65275	37.78683	37.65175	37.78693	37.65287	101	12	112	1763
AI_046_DSH	38.09616	37.88732	38.09566	37.88783	38.09594	37.88746	71	26	46	1215
AI_047_MLT	38.34962	38.34019	38.34966	38.34090	38.34974	38.34095	71	77	9	984
AI_048_ELZ	38.67043	39.19267	38.66960	39.19226	38.66977	39.19188	93	103	42	1071
AI_049_BNG	38.89708	40.50320	38.89743	40.50371	38.89721	40.50375	62	57	22	1133
AI_050_SLH_OE	38.96768	41.05361	38.96758	41.05301	38.96763	41.05309	61	52	9	1382

Table A.3 (Cont'd)

Station Code	Seis. Latitude	Seis. Longitude	CSL Latitude	CSL Longitude	Borehole Latitude	Borehole Longitude	Distance btw. Seis. and CSL (m)	Distance btw. Seis. and Borehole (m)	Distance btw. Borehole and CSL (m)	Altitude (m)
AI_051_SLH_MET	38.96604	41.04993	38.96646	41.05000	38.96657	41.05019	43	59	22	1383
AI_052_MUS	38.76111	41.50394	38.76091	41.50336	38.76093	41.50402	61	20	66	1303
AI_053_MLZ	39.14394	42.53072	39.14391	42.53003	39.14375	42.53023	69	53	26	1519
AI_054_TAT	38.50311	42.28097	38.50345	42.28136	38.50326	42.28129	52	35	20	1676
AI_055_VAN	38.50347	43.40177	38.50358	43.40123	38.50364	43.40145	55	36	23	1745
AI_056_MUR	38.99011	43.76302	38.99098	43.76368	38.99028	43.76318	109	23	86	1712
AI_057_DBY	39.54926	44.09089	39.54945	44.09011	39.54950	44.09078	80	26	67	1593
AI_058_AGR	39.71978	43.01640	39.71940	43.01503	39.71976	43.01630	142	10	132	1647
AI_059_HRS	40.04153	42.17355	40.04103	42.17220	40.04144	42.17331	144	26	118	1545
AI_060_KRS	40.60276	43.08207	40.60260	43.08165	40.60259	43.08210	45	17	45	1763
AI_061_ARD	41.10605	42.70493	41.10585	42.70496	41.10630	42.70497	20	25	45	1831
AI_062_ERZ	39.90316	41.26196	39.90315	41.26211	39.90321	41.26172	15	25	39	1908
AI_063_TER_MET	39.77672	40.39095	39.77693	40.39116	39.77678	40.39116	30	22	15	1435
AI_064_TER_PTT	39.77674	40.38386	-	-	39.77666	40.38383	-	9	-	1429
AI_065_ERC	39.74183	39.51152	39.74185	39.51190	39.74147	39.51173	38	42	42	1198
AI_066_ZAR	39.89281	37.74792	39.89281	37.74803	39.89284	37.74787	11	6	16	1349
AI_067_REF_HK	39.89934	38.76851	39.89943	38.76858	39.89921	38.76871	11	24	26	1587
AI_068_REF_KM	39.90507	38.77140	39.90491	38.77163	39.90488	38.77164	28	31	3	1579
AI_069_SSH	40.16928	38.10632	40.16921	38.10663	40.16920	38.10664	32	33	1	966
AI_070_RES	40.39440	37.32909	40.39390	37.32761	40.39380	37.32763	156	158	10	485
AI_071_TKT	40.32915	36.55522	40.32916	36.55423	40.32932	36.55470	99	55	50	590
AI_072_ERB	40.69804	36.56921	40.69831	36.56885	40.69814	36.56888	45	34	17	198
AI_073_AMS_MZFL	40.64382	35.80388	40.64413	35.80408	40.64391	35.80407	37	21	22	405
AI_074_AMS_BAY	40.66831	35.85278	40.66826	35.85278	40.66804	35.85255	5	35	32	419
AI_075_MRZ	40.87969	35.45884	40.87940	35.45875	40.87938	35.45883	30	31	8	757

Table A.3 (Cont'd)

Station Code	Seis. Latitude	Seis. Longitude	CSL Latitude	CSL Longitude	Borehole Latitude	Borehole Longitude	Distance btw. Seis. and CSL (m)	Distance btw. Seis. and Borehole (m)	Distance btw. Borehole and CSL (m)	Altitude (m)
AI_076_OSM_BEL	40.97142	34.79884	40.97135	34.79891	40.97139	34.79861	10	23	30	411
AI_077_OSM_EHK	40.97625	34.80015	40.97618	34.80063	40.97609	34.80041	49	31	24	422
AI_078_KRG	41.13945	34.48446	41.13966	34.48413	41.13981	34.48420	39	44	17	447
AI_079_TOS	41.01319	34.03671	41.01365	34.03638	41.01331	34.03681	57	16	55	873
AI_080_YLV	40.65870	29.27955	40.65855	29.28000	40.65848	29.27999	47	49	7	3
AI_081_IZN_KY	40.44163	29.71688	40.44196	29.71665	40.44237	29.71673	40	76	42	92
AI_082_CEK	41.02646	28.75870	41.02676	28.75863	41.02673	28.75872	31	27	9	55
AI_083_ERG	40.97297	27.95033	40.97330	27.95065	40.97301	27.95037	46	6	40	15
AI_084_TKR_MET	40.95820	27.49660	40.95808	27.49593	40.95862	27.49641	68	46	72	2
AI_085_TKR_HK	40.97928	27.51504	40.97918	27.51498	40.97936	27.51484	12	22	23	42
AI_086_SRK	40.61495	27.12252	40.61531	27.12296	40.61532	27.12276	57	44	20	10
AI_087_GL1	40.42334	26.66715	40.42323	26.66698	40.42330	26.66728	20	14	31	40
AI_088_CNK	40.14145	26.39948	40.14153	26.39966	40.14153	26.39939	20	12	27	1
AI_089_KRB	40.40421	27.30613	40.40433	27.30678	40.40427	27.30650	66	37	29	6
AI_090_BGA	40.23182	27.26288	40.23181	27.26288	40.23166	27.26245	1	46	46	24
AI_091_GNN	40.11399	27.64236	40.11393	27.64231	40.11396	27.64231	8	6	3	33
AI_092_EDN_SO	40.33601	27.86104	40.33585	27.86143	40.33590	27.86113	42	14	30	174
AI_093_EDN_KGI	40.34648	27.86182	40.34671	27.86198	40.34657	27.86184	28	9	20	257
AI_094_YNC	39.92916	27.25908	39.92946	27.25936	39.92926	27.25870	41	39	69	275
AI_095_EZN	39.77388	26.34563	39.77436	26.34540	39.77407	26.34556	53	20	33	68
AI_096_EDR	39.58952	27.01924	39.58943	27.01873	39.58934	27.01919	52	19	47	22
AI_097_AYV	39.31134	26.68601	39.31123	26.68623	39.31116	26.68624	25	29	7	4
AI_098_DKL	39.07390	26.88834	39.07393	26.88845	39.07324	26.88812	11	70	76	2
AI_099_KNK	39.08830	27.37472	39.08821	27.37463	39.08836	27.37465	13	9	15	71
AI_100_AKS	38.91121	27.82326	38.91126	27.82333	38.91138	27.82336	9	20	12	94

Table A.3 (Cont'd)

Station Code	Seis. Latitude	Seis. Longitude	CSL Latitude	CSL Longitude	Borehole Latitude	Borehole Longitude	Distance btw. Seis. and CSL (m)	Distance btw. Seis. and Borehole (m)	Distance btw. Borehole and CSL (m)	Altitude (m)
AI_101_GOR	38.93987	28.28315	38.93965	28.28280	38.93969	28.28327	41	22	47	670
AI_102_DMR	39.03503	28.64812	39.03495	28.64890	39.03503	28.64875	78	63	17	853
AI_103_SMV	39.09282	28.97848	39.09271	28.97870	39.09278	28.97892	25	44	23	828
AI_104_GDZ	38.99478	29.40040	38.99428	29.40041	38.99480	29.40020	50	20	56	735
AI_105_USK	38.67128	29.40401	38.67123	29.40415	38.67132	29.40393	15	9	24	920
AI_106_BLD	38.04483	28.83359	38.04491	28.83331	38.04489	28.83333	29	27	3	621
AI_107_DNZ_MET	37.76219	29.09222	37.76203	29.09228	37.76178	29.09233	17	42	25	427
AI_108_DNZ_BAY	37.81247	29.11113	37.81238	29.11111	37.81269	29.11086	9	35	40	332
AI_109_ALA	38.35556	28.51561	38.35520	28.51544	38.35554	28.51531	40	30	36	200
AI_110_SAL	38.48311	28.12347	38.48341	28.12317	38.48301	28.12376	42	31	71	111
AI_111_ODM	38.21565	27.96450	38.21556	27.96411	38.21561	27.96432	40	18	22	112
AI_112_MNS	38.61259	27.38138	38.61226	27.38156	38.61245	27.38112	38	30	48	106
AI_113_FOC	38.66241	26.75856	38.66240	26.75870	38.66228	26.75865	14	16	13	13
AI_114_GZL_MET	38.39443	27.08211	38.39465	27.08186	38.39450	27.08226	33	17	43	26
AI_115_BRN_BAY	38.45937	27.16689	38.45936	27.16688	38.45924	27.16607	1	83	82	15
AI_116_BRN_EU	38.45514	27.22673	38.45513	27.22700	38.45541	27.22575	27	102	128	35
AI_117_KUS_MET	37.85997	27.26501	37.85973	27.26513	37.85999	27.26530	27	29	31	24
AI_118_KUS_HSL	37.86200	27.26033	37.86203	27.26025	37.86229	27.26021	9	31	26	6
AI_119_AYD_HH	37.83657	27.83812	37.83635	27.83814	37.83680	27.83822	22	25	46	46
AI_120_AYD_DSI	37.84548	27.79956	37.84528	27.79965	37.84571	27.79938	22	29	51	65
AI_121_BDR	37.03304	27.43997	37.03300	27.43981	37.03257	27.43982	16	49	43	25
AI_122_MLS	37.30286	27.78059	37.30291	27.78016	37.30283	27.78028	43	31	14	55
AI_123_YTG	37.33967	28.13692	37.33981	28.13710	37.33976	28.13689	23	9	22	684
AI_124_YER	37.13378	28.28421	37.13441	28.28441	37.13451	28.28377	66	85	65	661
AI_125_MAR	36.83942	28.24483	36.83946	28.24471	36.83981	28.24478	13	39	36	19

Table A.3 (Cont'd)

Station Code	Seis. Latitude	Seis. Longitude	CSL Latitude	CSL Longitude	Borehole Latitude	Borehole Longitude	Distance btw. Seis. and CSL (m)	Distance btw. Seis. and Borehole (m)	Distance btw. Borehole and CSL (m)	Altitude (m)
AI_126_KOY	36.96996	28.68684	36.96955	28.68638	36.96963	28.68670	62	36	33	24
AI_127_FTH	36.62639	29.12399	36.62663	29.12376	36.62678	29.12398	33	39	27	3
AI_128_CAM	37.07411	29.34636	37.07353	29.34641	37.07393	29.34642	58	19	40	1297
AI_129_FNK	36.30219	30.14628	36.30220	30.14598	36.30226	30.14608	30	21	12	1
AI_130_BCK_KGI	37.46004	30.58844	37.45988	30.58811	37.45988	30.58881	37	40	70	850
AI_131_BCK_OM	37.45820	30.58761	37.45806	30.58766	37.45822	30.58765	15	4	16	803
AI_132_TFN	37.31607	29.77900	37.31618	29.77903	37.31627	29.77877	11	30	28	1153
AI_133_BRD1	37.72197	30.29399	37.72208	30.29413	37.72216	30.29405	18	20	11	957
AI_134_BRD2	37.70354	30.22084	37.70350	30.22061	37.70324	30.22073	23	32	29	874
AI_135_SNK	38.10476	30.55758	38.10471	30.55790	38.10468	30.55758	32	8	32	970
AI_136_CRD	37.82446	29.66813	37.82336	29.66733	37.82452	29.66815	136	6	142	863
AI_137_DIN	38.05990	30.15373	38.05991	30.15346	38.05999	30.15353	27	22	11	862
AI_138_SDL	38.43701	30.25245	38.43695	30.25236	38.43740	30.25253	11	40	48	1056
AI_139_AFY	38.77598	30.53395	38.77635	30.53391	38.77620	30.53451	37	60	62	1054
AI_140_STG	39.44626	30.69658	39.44630	30.69653	39.44621	30.69651	6	9	9	999
AI_141_KUT_BAY	39.42779	29.99155	39.42821	29.99176	39.42780	29.99160	47	5	44	932
AI_142_KUT_SS	39.41930	29.99716	39.41933	29.99698	39.41864	29.99715	18	66	71	938
AI_143_EMT	39.33546	29.24982	39.33530	29.25003	39.33564	29.24968	26	23	49	853
AI_144_DUR_MET	39.57798	28.63232	39.57753	28.63216	39.57803	28.63266	48	34	71	649
AI_145_DUR_KGI	39.60408	28.62655	39.60448	28.62640	39.60419	28.62642	43	17	29	690
AI_146_BLK	39.65003	27.85686	39.64986	27.85701	39.64999	27.85722	23	36	25	262
AI_147_BGC	39.39786	28.12733	39.39810	28.12803	39.39834	28.12792	74	76	26	148
AI_148_SNG	39.25458	28.16439	39.25435	28.16532	39.25451	28.16432	96	10	101	217
AI_149_BND_MET	40.33193	27.99662	40.33216	27.99680	40.33201	27.99676	29	16	16	61
AI_150_BND_TDM	40.34135	27.94225	40.34156	27.94176	40.34157	27.94163	53	66	13	90

Table A.3 (Cont'd)

Station Code	Seis. Latitude	Seis. Longitude	CSL Latitude	CSL Longitude	Borehole Latitude	Borehole Longitude	Distance btw. Seis. and CSL (m)	Distance btw. Seis. and Borehole (m)	Distance btw. Borehole and CSL (m)	Altitude (m)
AI_151_MKP	40.03471	28.39392	40.03431	28.39464	40.03463	28.39400	82	11	72	41
AI_152_BYT02	40.22566	29.07518	40.22590	29.07443	40.22592	29.07570	79	58	127	91
AI_153_ING	40.06708	29.50882	40.06713	29.50865	40.06725	29.50824	18	60	43	304

Table A.4 Site Properties of the Stations

Station Code	GWL (m)	$V_{s,30}$ (m/s)	N_{mean}	Site Class NEHRP V_s Criteria	Site Class NEHRP SPT Criteria	Site Class EC-8 V_s Criteria	Site Class EC-8 SPT Criteria	Site Class TSDC V_s Criteria	Site Class TSDC SPT Criteria
AI_001_IST	NA	595.2	100.0	C	C	B	B	Z3	-
AI_002_GBZ	NA	701.1	100.0	C	C	B	B	Z2	-
AI_003_IZN	4.8	251.2	12.3	D	E	C	D	Z3	Z3
AI_004_IZT	NA	826.1	100.0	B	C	A	B	Z2	-
AI_005_SKR	NA	412.0	55.9	C	C	B	B	Z3	Z1
AI_006_AKY	6.7	271.6	22.8	D	D	C	C	Z3	Z3
AI_007_GYN_BHM	12.4	471.7	39.3	C	D	B	C	Z3	-
AI_008_GYN_DH	9.5	347.7	21.0	D	D	C	C	Z3	Z3
AI_009_MDR	10.8	355.4	48.6	D	D	C	C	Z2	Z2
AI_010_BOL	2.7	293.6	29.5	D	D	C	C	Z3	Z1
AI_011_DZC	6.3	282.0	31.0	D	D	C	C	Z3	Z3
AI_012_MEN	3.7	364.7	21.1	C	D	B	C	Z3	Z3
AI_013_CER	4.5	347.9	41.0	D	D	C	C	Z2	-
AI_014_KBK	NA	702.6	100.0	C	C	B	B	Z3	-
AI_015_GRD	8.2	444.7	77.3	C	C	B	B	Z3	-
AI_016_BEY	19.5	339.6	51.9	D	C	C	B	Z2	Z2
AI_017_HAY	NA	418.8	100.0	C	C	B	B	Z3	-
AI_018_CMR	6.3	312.5	51.4	D	C	C	B	Z3	-
AI_019_MRS	2.4	366.4	25.5	C	D	B	C	Z2	Z2
AI_020_KRT	7.3	485.1	95.3	C	C	B	B	Z2	-
AI_021_CYH_PTT	3.1	223.0	16.5	D	D	C	C	Z4	Z2
AI_022_CYH_TIM	3.2	263.8	16.3	D	D	C	C	Z3	Z2
AI_023_MAT17	4.3	349.9	51.7	D	C	C	B	Z2	Z2
AI_024_MAT18	NA	430.4	100.0	C	C	B	B	Z3	-
AI_025_MAT06_MET	2.3	395.2	29.7	C	D	B	C	Z2	Z2

Table A.4 (Cont'd)

Station Code	GWL (m)	$V_{s,30}$ (m/s)	N_{mean}	Site Class NEHRP V_s Criteria	Site Class NEHRP SPT Criteria	Site Class EC-8 V_s Criteria	Site Class EC-8 SPT Criteria	Site Class TSDC V_s Criteria	Site Class TSDC SPT Criteria
AI_026_MAT06_MIM	10.7	309.6	42.9	D	D	C	C	Z3	Z2
AI_027_MAT01	3.2	209.6	28.1	D	D	C	C	Z3	Z2
AI_028_MAT03	13.5	469.5	76.3	C	C	B	B	Z2	-
AI_029_MAT02	NA	343.6	59.9	D	C	C	B	Z3	-
AI_030_MAT04	NA	338.3	42.8	D	D	C	C	Z2	Z2
AI_031_MAT05	NA	539.2	100.0	C	C	B	B	Z2	-
AI_032_MAT07	20.2	271.6	19.8	D	D	C	C	Z3	Z3
AI_033_MAT08	NA	688.0	100.0	C	C	B	B	Z2	-
AI_034_MAT09	NA	618.0	100.0	C	C	B	B	Z2	-
AI_035_MAT15	NA	420.9	97.2	C	C	B	B	Z2	-
AI_036_MAT16	13.5	598.9	93.0	C	C	B	B	Z2	-
AI_037_MAT13	NA	390.5	34.1	C	D	B	C	Z2	Z2
AI_038_MAT14	23.6	484.4	100.0	C	C	B	B	Z2	-
AI_039_AND	8.3	610.8	44.3	C	D	B	C	Z2	-
AI_040_ELB	5.3	314.9	33.9	D	D	C	C	Z3	Z2
AI_041_MAT11	10.2	345.5	58.6	D	C	C	B	Z3	Z1
AI_042_MAT12_MET	NA	316.7	36.8	D	D	C	C	Z3	Z1
AI_043_KMR	NA	466.2	77.1	C	C	B	B	Z2	-
AI_044_MAT10	NA	671.1	100.0	C	C	B	B	Z2	-
AI_045_GOL	2.3	468.7	40.8	C	D	B	C	Z3	-
AI_046_DSH	NA	654.4	100.0	C	C	B	B	Z2	-
AI_047_MLT	NA	480.8	62.5	C	C	B	B	Z3	-
AI_048_ELZ	NA	407.3	82.7	C	C	B	B	Z3	-
AI_049_BNG	6.5	528.7	96.8	C	C	B	B	Z2	-
AI_050_SLH_OE	5.4	484.8	44.4	C	D	B	C	Z2	Z2

Table A.4 (Cont'd)

Station Code	GWL (m)	$V_{s,30}$ (m/s)	N_{mean}	Site Class NEHRP V_s Criteria	Site Class NEHRP SPT Criteria	Site Class EC-8 V_s Criteria	Site Class EC-8 SPT Criteria	Site Class TSDC V_s Criteria	Site Class TSDC SPT Criteria
AI_051_SLH_MET	6.5	462.7	55.3	C	C	B	B	Z2	Z1
AI_052_MUS	11.2	314.5	22.6	D	D	C	C	Z3	Z3
AI_053_MLZ	NA	311.2	31.0	D	D	C	C	Z3	Z1
AI_054_TAT	11.3	273.0	36.4	D	D	C	C	Z3	-
AI_055_VAN	NA	363.1	37.4	C	D	B	C	Z3	Z1
AI_056_MUR	7.3	292.6	16.7	D	D	C	C	Z3	Z2
AI_057_DBY	NA	270.7	22.7	D	D	C	C	Z3	Z2
AI_058_AGR	7.3	294.8	29.0	D	D	C	C	Z3	Z2
AI_059_HRS	NA	316.4	49.4	D	D	C	C	Z3	Z1
AI_060_KRS	6.7	269.7	21.5	D	D	C	C	Z3	Z3
AI_061_ARD	NA	431.7	70.6	C	C	B	B	Z2	-
AI_062_ERZ	NA	374.9	79.5	C	C	B	B	Z2	Z1
AI_063_TER_MET	16.3	319.6	23.1	D	D	C	C	Z3	Z2
AI_064_TER_PTT	10.5	349.8	56.3	D	C	C	B	Z2	Z1
AI_065_ERC	10.2	314.2	17.4	D	D	C	C	Z3	Z2
AI_066_ZAR	16.5	281.6	19.1	D	D	C	C	Z3	Z2
AI_067_REF_HK	8.1	433.1	26.5	C	D	B	C	Z2	Z3
AI_068_REF_KM	NA	413.1	57.8	C	C	B	B	Z2	Z2
AI_069_SSH	11.4	413.4	81.4	C	C	B	B	Z2	-
AI_070_RES	5.7	376.2	80.5	C	C	B	B	Z2	-
AI_071_TKT	6.3	323.8	54.3	D	C	C	B	Z2	Z1
AI_072_ERB	2.1	326.6	56.7	D	C	C	B	Z3	Z1
AI_073_AMS_MZFL	5.5	283.9	35.7	D	D	C	C	Z3	Z2
AI_074_AMS_BAY	11.4	443.3	84.4	C	C	B	B	Z3	-
AI_075_MRZ	NA	368.4	40.9	C	D	B	C	Z3	Z2

Table A.4 (Cont'd)

Station Code	GWL (m)	$V_{s,30}$ (m/s)	N_{mean}	Site Class NEHRP V_s Criteria	Site Class NEHRP SPT Criteria	Site Class EC-8 V_s Criteria	Site Class EC-8 SPT Criteria	Site Class TSDC V_s Criteria	Site Class TSDC SPT Criteria
AI_076_OSM_BEL	4.3	314.9	43.9	D	D	C	C	Z3	Z2
AI_077_OSM_EHK	2.5	254.6	14.9	D	E	C	D	Z3	Z2
AI_078_KRG	NA	687.8	100.0	C	C	B	B	Z1	-
AI_079_TOS	NA	361.8	76.2	C	C	B	B	Z2	-
AI_080_YLV	3.4	261.2	30.0	D	D	C	C	Z3	-
AI_081_IZN_KY	0	196.7	3.3	D	E	C	D	Z4	Z3
AI_082_CEK	NA	283.3	33.0	D	D	C	C	Z3	Z1
AI_083_ERG	5.5	325.2	28.8	D	D	C	C	Z3	Z3
AI_084_TKR_MET	2.1	471.9	97.5	C	C	B	B	Z3	-
AI_085_TKR_HK	NA	408.7	100.0	C	C	B	B	Z3	-
AI_086_SRK	5.5	225.0	20.2	D	D	C	C	Z4	Z3
AI_087_GL1	NA	285.9	81.8	D	C	C	B	Z3	Z1
AI_088_CNK	1.2	191.8	18.6	D	D	C	C	Z4	Z3
AI_089_KRB	NA	683.2	95.9	C	C	B	B	Z2	-
AI_090_BGA	NA	303.7	47.9	D	D	C	C	Z3	Z2
AI_091_GNN	1.7	397.2	83.9	C	C	B	B	Z3	-
AI_092_EDN_SO	23.5	330.0	50.1	D	C	C	B	Z2	Z2
AI_093_EDN_KGI	NA	520.1	100.0	C	C	B	B	Z3	-
AI_094_YNC	NA	324.1	49.8	D	D	C	C	Z3	Z1
AI_095_EZN	NA	403.2	82.6	C	C	B	B	Z2	Z1
AI_096_EDR	10.5	223.3	37.4	D	D	C	C	Z4	Z2
AI_097_AYV	NA	386.6	43.2	C	D	B	C	Z3	-
AI_098_DKL	2.3	193.2	10.7	D	E	C	D	Z3	Z4
AI_099_KNK	NA	558.0	68.2	C	C	B	B	Z2	-
AI_100_AKS	4.5	291.7	18.8	D	D	C	C	Z3	Z2

Table A.4 (Cont'd)

Station Code	GWL (m)	$V_{s,30}$ (m/s)	N_{mean}	Site Class NEHRP V_s Criteria	Site Class NEHRP SPT Criteria	Site Class EC-8 V_s Criteria	Site Class EC-8 SPT Criteria	Site Class TSDC V_s Criteria	Site Class TSDC SPT Criteria
AI_101_GOR	NA	629.4	100.0	C	C	B	B	Z2	-
AI_102_DMR	NA	335.8	92.7	D	C	C	B	Z3	-
AI_103_SMV	3.6	259.0	19.4	D	D	C	C	Z3	Z2
AI_104_GDZ	NA	343.2	65.9	D	C	C	B	Z3	-
AI_105_USK	NA	285.5	24.8	D	D	C	C	Z3	Z2
AI_106_BLD	NA	345.4	84.2	D	C	C	B	Z3	-
AI_107_DNZ_MET	NA	345.9	33.1	D	D	C	C	Z2	Z2
AI_108_DNZ_BAY	5.5	355.9	91.7	D	C	C	B	Z3	-
AI_109_ALA	NA	358.1	42.1	D	D	C	C	Z3	Z2
AI_110_SAL	10.7	272.9	29.4	D	D	C	C	Z3	Z2
AI_111_ODM	NA	286.3	25.6	D	D	C	C	Z3	Z2
AI_112_MNS	NA	340.3	46.8	D	D	C	C	Z2	Z2
AI_113_FOC	9.6	327.7	43.5	D	D	C	C	Z3	Z2
AI_114_GZL_MET	NA	770.7	100.0	B	C	B	B	Z2	-
AI_115_BRN_BAY	3.5	195.5	7.4	D	E	C	D	Z4	Z3
AI_116_BRN_EU	7	270.0	33.8	D	D	C	C	Z3	Z2
AI_117_KUS_MET	NA	369.3	100.0	C	C	B	B	Z3	-
AI_118_KUS_HSL	1.3	273.5	13.8	D	E	C	D	Z3	Z3
AI_119_AYD_HH	NA	310.9	44.4	D	D	C	C	Z2	Z1
AI_120_AYD_DSI	NA	271.4	38.5	D	D	C	C	Z3	Z2
AI_121_BDR	NA	746.9	100.0	C	C	B	B	Z2	-
AI_122_MLS	19	323.5	30.9	D	D	C	C	Z3	Z2
AI_123_YTG	NA	695.9	100.0	C	C	B	B	Z2	-
AI_124_YER	NA	813.4	100.0	B	C	A	B	Z2	-
AI_125_MAR	12.3	392.5	52.8	C	C	B	B	Z3	Z1

Table A.4 (Cont'd)

Station Code	GWL (m)	$V_{s,30}$ (m/s)	N_{mean}	Site Class NEHRP V_s Criteria	Site Class NEHRP SPT Criteria	Site Class EC-8 V_s Criteria	Site Class EC-8 SPT Criteria	Site Class TSDC V_s Criteria	Site Class TSDC SPT Criteria
AI_126_KOY	NA	371.9	25.2	C	D	B	C	Z2	Z2
AI_127_FTH	0.7	248.2	19.5	D	D	C	C	Z3	Z2
AI_128_CAM	NA	344.1	100.0	D	C	C	B	Z3	-
AI_129_FNK	0.5	299.4	27.0	D	D	C	C	Z3	Z2
AI_130_BCK_KGI	NA	713.7	100.0	C	C	B	B	Z3	-
AI_131_BCK_OM	NA	693.8	100.0	C	C	B	B	Z1	-
AI_132_TFN	NA	366.9	71.5	C	C	B	B	Z2	Z1
AI_133_BRD1	16.5	334.6	48.9	D	D	C	C	Z2	Z1
AI_134_BRD2	11.8	294.1	36.4	D	D	C	C	Z3	Z2
AI_135_SNK	NA	445.1	50.3	C	C	B	B	Z2	Z2
AI_136_CRD	25.5	395.1	63.9	C	C	B	B	Z3	Z1
AI_137_DIN	2.3	198.1	15.9	D	D	C	C	Z4	Z2
AI_138_SDL	17.2	357.4	46.4	D	D	C	C	Z2	Z2
AI_139_AFY	5.1	225.6	17.3	D	D	C	C	Z3	Z3
AI_140_STG	4.3	407.4	35.1	C	D	B	C	Z3	-
AI_141_KUT_BAY	2.8	266.6	6.9	D	E	C	D	Z3	Z3
AI_142_KUT_SS	3.2	242.5	10.2	D	E	C	D	Z4	Z3
AI_143_EMT	NA	303.6	19.0	D	D	C	C	Z3	Z2
AI_144_DUR_MET	NA	560.7	100.0	C	C	B	B	Z2	-
AI_145_DUR_KGI	NA	495.9	100.0	C	C	B	B	Z3	-
AI_146_BLK	NA	662.0	100.0	C	C	B	B	Z2	-
AI_147_BGC	3.4	299.9	31.5	D	D	C	C	Z3	Z1
AI_148_SNG	3.7	237.7	19.5	D	D	C	C	Z3	Z3
AI_149_BND_MET	NA	321.0	38.2	D	D	C	C	Z2	Z1
AI_150_BND_TDM	NA	416.7	75.2	C	C	B	B	Z2	Z1

Table A.4 (Cont'd)

Station Code	GWL (m)	$V_{s,30}$ (m/s)	N_{mean}	Site Class NEHRP V_s Criteria	Site Class NEHRP SPT Criteria	Site Class EC-8 V_s Criteria	Site Class EC-8 SPT Criteria	Site Class TSDC V_s Criteria	Site Class TSDC SPT Criteria
AI_151_MKP	NA	264.9	47.7	D	D	C	C	Z3	Z2
AI_152_BYT02	3.2	249.1	21.2	D	D	C	C	Z3	Z3
AI_153_ING	4.5	252.0	27.4	D	D	C	C	Z3	Z2

APPENDIX B

SITES THAT ARE SUSCEPTIBLE TO LIQUEFACTION

Table B.1 Sites that are susceptible to liquefaction

Station Code	GWL	Total Thickness of Liq. Soils	Av. Depth (m)	Sample Type	a_{crt} (g)
AI_003_IZN	4.8	7.5	6.30	SPT-4	0.17
AI_003_IZN	4.8	7.5	9.30	SPT-6	0.40
AI_003_IZN	4.8	7.5	10.80	SPT-7	0.24
AI_003_IZN	4.8	7.5	12.30	SPT-8	0.35
AI_003_IZN	4.8	7.5	13.80	SPT-9	0.29
AI_012_MEN	3.7	1.5	4.80	SPT-3	0.37
AI_018_CMR	6.3	1.5	6.30	SPT-4	0.48
AI_023_MAT17	4.3	1.5	4.80	SPT-3	0.37
AI_025_MAT06_MET	2.3	4.5	12.30	SPT-5	0.19
AI_025_MAT06_MET	2.3	4.5	13.80	SPT-6	0.16
AI_025_MAT06_MET	2.3	4.5	15.30	SPT-7	0.20
AI_027_MAT01	3.2	3	10.80	SPT-7	0.50
AI_027_MAT01	3.2	3	15.30	SPT-10	0.49
AI_050_SLH_OE	5.4	3	6.30	SPT-4	0.61
AI_050_SLH_OE	5.4	3	7.80	SPT-5	0.50
AI_052_MUS	11.2	1.5	15.30	SPT-10	0.26
AI_056_MUR	7.3	4.5	7.80	SPT-5	0.28
AI_056_MUR	7.3	4.5	9.30	SPT-6	0.23
AI_056_MUR	7.3	4.5	10.80	SPT-7	0.25
AI_058_AGR	7.3	1.5	10.80	SPT-7	0.29
AI_065_ERC	10.2	4.5	12.30	SPT-8	0.37
AI_065_ERC	10.2	4.5	13.80	SPT-9	0.37
AI_065_ERC	10.2	4.5	15.30	SPT-10	0.70
AI_073_AMS_MZFL	5.5	1.5	6.30	SPT-2	0.35
AI_080_YLV	3.4	3	4.80	SPT-3	0.39
AI_080_YLV	3.4	3	6.30	SPT-4	0.21
AI_081_IZN_KY	0	6	1.80	SPT-1	0.05
AI_081_IZN_KY	0	6	3.30	SPT-2	0.13
AI_081_IZN_KY	0	6	10.80	SPT-7	0.17

Table B.1 (Cont'd)

Station Code	GWL	Total Thickness of Liq. Soils	Av. Depth (m)	Sample Type	a_{crt} (g)
AI_081_IZN_KY	0	6	13.80	SPT-9	0.11
AI_083_ERG	5.5	1.5	6.30	SPT-4	0.22
AI_086_SRK	5.5	1.5	7.80	SPT-5	0.39
AI_088_CNK	1.2	10.5	1.80	SPT-1	0.30
AI_088_CNK	1.2	10.5	3.30	SPT-2	0.11
AI_088_CNK	1.2	10.5	4.80	SPT-3	0.08
AI_088_CNK	1.2	10.5	10.80	SPT-7	0.40
AI_088_CNK	1.2	10.5	12.30	SPT-8	0.26
AI_088_CNK	1.2	10.5	13.80	SPT-9	0.28
AI_088_CNK	1.2	10.5	15.30	SPT-10	0.39
AI_098_DKL	2.3	9	3.30	SPT-2	0.24
AI_098_DKL	2.3	9	4.80	SPT-3	0.25
AI_098_DKL	2.3	9	6.30	SPT-4	0.24
AI_098_DKL	2.3	9	7.80	SPT-5	0.15
AI_098_DKL	2.3	9	9.30	SPT-6	0.17
AI_098_DKL	2.3	9	10.80	SPT-7	0.12
AI_100_AKS	4.5	3	9.30	SPT-6	0.23
AI_100_AKS	4.5	3	12.30	SPT-8	0.18
AI_103_SMV	3.6	6	4.80	SPT-3	0.35
AI_103_SMV	3.6	6	6.30	SPT-4	0.13
AI_103_SMV	3.6	6	12.30	SPT-8	0.26
AI_103_SMV	3.6	6	13.80	SPT-9	0.26
AI_115_BRN_BAY	3.5	9	4.80	SPT-3	0.10
AI_115_BRN_BAY	3.5	9	6.30	SPT-4	0.10
AI_115_BRN_BAY	3.5	9	10.80	SPT-7	0.16
AI_115_BRN_BAY	3.5	9	12.30	SPT-8	0.30
AI_115_BRN_BAY	3.5	9	13.80	SPT-9	0.27
AI_115_BRN_BAY	3.5	9	15.30	SPT-10	0.12
AI_118_KUS_HSL	1.3	7.5	6.30	SPT-4	0.10
AI_118_KUS_HSL	1.3	7.5	9.30	SPT-6	0.12
AI_118_KUS_HSL	1.3	7.5	10.80	SPT-7	0.14
AI_118_KUS_HSL	1.3	7.5	13.80	SPT-9	0.11
AI_118_KUS_HSL	1.3	7.5	15.30	SPT-10	0.16
AI_127_FTH	0.7	1.5	10.80	SPT-7	0.39
AI_129_FNK	0.5	4.5	12.30	SPT-8	0.22
AI_129_FNK	0.5	4.5	13.80	SPT-9	0.28
AI_129_FNK	0.5	4.5	15.30	SPT-10	0.30
AI_139_AFY	5.1	9	7.80	SPT-5	0.41
AI_139_AFY	5.1	9	9.30	SPT-6	0.24
AI_139_AFY	5.1	9	10.80	SPT-7	0.32
AI_139_AFY	5.1	9	12.30	SPT-8	0.35
AI_139_AFY	5.1	9	13.80	SPT-9	0.26

Table B.1 (Cont'd)

Station Code	GWL	Total Thickness of Liq. Soils	Av. Depth (m)	Sample Type	a_{crt} (g)
AI_139_AFY	5.1	9	15.30	SPT-10	0.43
AI_141_KUT_BAY	2.8	3	10.80	SPT-7	0.43
AI_141_KUT_BAY	2.8	3	12.30	SPT-8	0.29
AI_142_KUT_SS	3.2	4.5	6.30	SPT-4	0.13
AI_142_KUT_SS	3.2	4.5	7.80	SPT-5	0.30
AI_142_KUT_SS	3.2	4.5	12.30	SPT-8	0.20
AI_148_SNG	3.7	9	7.80	SPT-5	0.34
AI_148_SNG	3.7	9	9.30	SPT-6	0.15
AI_148_SNG	3.7	9	10.80	SPT-7	0.44
AI_148_SNG	3.7	9	12.30	SPT-8	0.44
AI_148_SNG	3.7	9	13.80	SPT-9	0.27
AI_148_SNG	3.7	9	15.30	SPT-10	0.22
AI_152_BYT02	3.2	7.5	4.80	SPT-3	0.17
AI_152_BYT02	3.2	7.5	7.80	SPT-5	0.12
AI_152_BYT02	3.2	7.5	9.30	SPT-6	0.33
AI_152_BYT02	3.2	7.5	10.80	SPT-7	0.30
AI_152_BYT02	3.2	7.5	12.30	SPT-8	0.49
AI_153_ING	4.5	6	4.80	SPT-3	0.39
AI_153_ING	4.5	6	6.30	SPT-4	0.47
AI_153_ING	4.5	6	7.80	SPT-5	0.38
AI_153_ING	4.5	6	13.80	SPT-9	0.29